

FINITE ELEMENT ANALYSIS OF SOIL COMPACTION

by

George Edward Coleman, III

Thesis submitted to the Graduate Faculty of the
Virginia Polytechnic Institute and State University
in partial fulfillment of the requirements for the degree of

MASTER OF SCIENCE

in

Agricultural Engineering

APPROVED:

J. V. Perumpral, Chairman

M. E. Wright

J. P. H. Mason

November, 1972

Blacksburg, Virginia

ACKNOWLEDGEMENTS

The author wishes to express his gratitude to the Montgomery County School Board, the Environmental Systems Laboratories, and the Agricultural Engineering Department for employment opportunities which provided financial support during parts of this investigation.

Thanks go to the members of the author's committee, Drs. J. V. Perumpral, J. P. Mason, and M. E. Wright. Special thanks are extended to Dr. Perumpral whose ideas, criticisms, and reviews were invaluable in the investigation and the preparation of the manuscript. Also, appreciation is expressed to the staff of the Virginia Polytechnic Institute and State University Computing Center for advice and assistance during the analytical portion of the investigation.

Last, but not least, my deepest appreciation is expressed to my family who have endured many ordeals during this project and to my wife in particular whose love, understanding, patience, and typing helped to supply needed reassurance and support.

TABLE OF CONTENTS

<u>Subject</u>	<u>Page</u>
INTRODUCTION.....	1
REVIEW OF LITERATURE.....	3
Force Compaction Relationships.....	3
Numerical Methods.....	6
Triaxial Compression Test.....	10
FINITE ELEMENT ANALYSIS.....	11
Element Stiffness Matrix.....	12
System Stiffness Matrix.....	23
METHOD OF ANALYSIS.....	25
The Soil Sample.....	25
Stress-Strain Relationship.....	25
Non-Linear Analysis.....	28
Volumetric Strain.....	30
Finite Element Program.....	31
RESULTS AND DISCUSSION.....	32
Axial Strain in the Sample.....	33
Total Sample Volumetric Strain.....	35
Compaction Zones Within the Sample.....	40
CONCLUSIONS.....	45
RECOMMENDATIONS.....	46
BIBLIOGRAPHY.....	47
APPENDIX I - Finite Element Program.....	49
APPENDIX II - Sample Computer Output.....	67
VITA.....	72

LIST OF FIGURES

<u>Figure No.</u>	<u>Page</u>
1. Typical Axi-Symmetric System.....	13
2. Idealized Two Dimensional System.....	14
3. A Typical Rectangular Element in the Idealized System.....	15
4. Displaced Rectangular Element.....	17
5. Stresses on an Axi-Symmetric Element.....	20
6. Stress-Strain Relationship used for Finite Element Analysis.....	27
7. Comparison of Stress-Strain Relationships.....	34
8. Relationship Between Compaction and Mean Normal Stress.....	36
9. Relationship Between Compaction and Maximum Shear Stress.....	37
10. Relationship Between Mean Normal Stress and Maximum Shear Stress for Constant Volumetric Strain.....	39
11. Comparison of Compaction Determined by Finite Element Analysis and by the Relationship Developed.....	41
12a. Volumetric Strain Contours Within the Soil Sample.....	42
12b. Volumetric Strain Contours Within the Soil Sample.....	43

INTRODUCTION

Compaction is the action of changing the volume of a given mass of material. Soil compaction may then be thought of as the action of decreasing the volume of a given quantity of soil. The degree of compaction may be quantified as a change in bulk density, void ratio, porosity, or absolute volume, or as volumetric strain. Regardless of the measure, compaction is of major concern to those in the agricultural industry, for the following reasons.

Investigations have shown that the soil compaction increases the mechanical strength of the soil so that the root growth is impeded. Compaction changes the relative proportions of solids, air, and moisture in the three phase soil system. Compaction also decreases the infiltration rate of air and water into the soil so that smaller amounts of air, moisture, and plant nutrients reach the plant roots. Decreased water infiltration produces an increased run-off which provides more opportunity for erosion. These changes can have a significant influence upon seed germination, root development, plant growth, and thus affect total crop yield.

Soil compaction is caused by forces which act on the soil medium. These forces originate from two general sources, natural and mechanical. Natural forces are caused by rain, wind, freezing, and thawing. Mechanical forces are caused by animals and machines. The increased use of heavier equipment for planting, tillage, and harvesting operations is a primary contributing factor in causing soil compaction.

In order to prevent or control soil compaction which is undesirable in agriculture, one must be able to predict the amount of compaction which a particular soil will undergo for given loads. To predict the degree of compaction one needs to obtain a more complete understanding of the relationship between compaction and the forces which cause it.

Recognition of this need is reflected in the research which has been conducted to relate soil compaction to the force system. Based on experimental results, attempts have already been made to relate soil compaction to the major principal stress (1)*, to the mean or octahedral normal stress (2,6,12) and to the stress invariants (8). Some of the relationships include the effects of shear stress (2,6) or shear strain (14) which, at best, are difficult to measure even under laboratory conditions. Needless to say, it becomes practically impossible to obtain measures of these in the field.

The experimental approaches taken in the past have been laborious and time consuming. In recent years, with the high speed electronic computers becoming more easily accessible, use of numerical methods to solve complex boundary value problems has increased considerably. It might be possible to adapt one of these numerical techniques to study soil compaction. Therefore, the broad objective of this study is to consider the feasibility of adapting a numerical method to study force-compaction phenomena in soils.

*Numbers in parentheses indicate references to appended bibliography.

REVIEW OF LITERATURE

Force Compaction Relationships

The need for a better understanding of soil compaction has led many researchers to attempt to relate compaction to applied soil forces and resulting stresses. Soehne (12) used a small cylindrical container of soil to study the static and dynamic force effects on soil compaction. For the static tests a hydraulic ram was used to load the soil. The dynamic load was applied by using a spring loaded kneading apparatus. The spring was graduated so that a constant maximum force could be applied to the sample. From this study the porosity of the soil was related to the applied axial force by:

$$n = A^* \log(p) + C \quad [1]$$

where: A^* is the slope of the $\log(p)$ vs. n graph.

p is the applied axial pressure

C is the porosity at an axial pressure of 10 psi.

n is the porosity of the soil.

This is to say that the soil porosity, which indicates the compactness of the soil, may be related to the maximum principal stress.

Chancellor *et al.* (3) later concluded that compaction does not relate uniquely with the largest principal stress. In these tests, much larger cylindrical soil samples were loaded. Deformation and volumetric strain due to a load applied on the soil surface were determined using a lime and wet plaster grid system or by taking X-ray

photographs of lead shot movements. From a similar study Chancellor and Schmidt (4) found that the soil deformation, and thus the compaction, was influenced to some extent by shear deformations.

Based on continuum mechanics theories, Vanden Berg *et al.* (13) hypothesized that compaction was proportional to mean stress or the spherical stress tensor and theoretically not influenced by the deviatoric stress tensor. Vanden Berg (14) later concluded that the theories of continuum mechanics did not completely describe the soil deformation. He proposed that the soil compaction results from two types of soil reactions to the applied forces. First, the compression of the soil medium under load, which is theoretically related to the spherical stress tensor. Second, the rearrangement of the grains or soil particles to occupy less space. This rearrangement would be indicated by the shear deformation or shear strain. From the results of this study the relationship of compaction to normal stress and shear strain was:

$$BD = BD_0 + C\sigma_m (1 + \bar{\gamma}_{\max}) \quad [2]$$

where: BD is the bulk density of the soil (weight per unit vol.).

BD_0 is the original bulk density of the sample.

σ_m is the mean (octahedral) normal stress

$\bar{\gamma}_{\max}$ is the principal natural shear strain.

C is a soil parameter.

Vanden Berg concluded that the proposed hypothesis of compaction being the result of compression and reorientation was valid, but for practical

usefulness the maximum shear strain must be related to the state of stress.

Harris *et al.* (8) tried to relate volumetric strain to mean normal stress, maximum principal stress, deviatoric stress, and maximum shear stress. They found best correlation with the maximum shear stress, while the results of the relationship of volumetric strain to mean normal stress were inconclusive.

Bailey and Vanden Berg (2) proposed a soil compaction yield surface described by the following relationships:

$$BWV = m \log \left(\sqrt{\sigma_m^2 + \tau_{\max}^2} \right) + n \left(\frac{\tau_{\max}}{\sigma_m} \right) + BWV_o \quad [3]$$

where: σ_m is the mean normal stress.

τ_{\max} is the maximum shear stress.

BWV is the bulk weight volume of the sample (volume per unit wt).

BWV_o is the original BWV of the sample.

m and n are material parameters.

Bailey (1) later showed the concept of this compaction surface on the yield diagram to be invalid because triaxial samples which were pre-compacted to different stress levels had different strengths.

Dunlap and Weber (6) developed a relationship from the results of triaxial tests in which a soil sample in the shape of a parallelepiped was acted upon by a general force system. During the tests normal loads acting on the specimen could be varied independently of each

other. From the results of this study the following relationship was developed:

$$BWW = BWV_o + m \ln(\sigma_m) \frac{\tau_{max}}{a\sigma_m + b}$$

where: σ_m is the mean normal stress.

τ_{max} is the maximum shear stress.

BWV is the bulk weight volume of the sample.

BWV_o is the original bulk weight volume of the sample.

m , a and b are material parameters.

Note in the above equation when the sample is hydrostatically loaded, that is, when the three normal loads applied are equal, the shear stress becomes zero and the last term drops from the equation.

Numerical Methods

The two numerical methods generally used for solving boundary value problems are the finite difference method and the finite element technique. Christian (5) utilized the finite difference method to study stress and strain distribution in soils, due to a surface load, using plastic strain increment. However, recent advancements in structural analysis have led to the development of a relatively versatile technique known as the finite element method. This method of analysis offers several distinctive advantages over techniques previously employed.

With the finite element method the continuum can be approximated by a finite number of elements, thus the name finite element. The accuracy of the solution may be increased by decreasing the size of

the elements. In two dimensional analysis these elements may be triangles or quadrilaterals of varying sizes. These elements can be assembled to approximate irregular boundaries and geometric discontinuities. Elements may be of different materials with anisotropic strength properties. Boundary loads may be applied at any internal or external node in the continuum as forces, displacements, thermal and acceleration loads. Many of these things could be included in other numerical methods, but the programming and computation time which would be required makes their inclusion prohibitive.

Girijavallabhan and Reese (7) employed the finite element method to obtain a load-settlement relationship for a rigid footing on a soft clay and a load-displacement relationship for a strip of long vertical wall retaining sand. In both problems the material response of the soil was considered to be non-linear, and the stress-strain relationship was expressed as:

$$\begin{aligned}\epsilon_o &= f(\sigma_o, \tau_o) \\ \gamma_o &= g(\sigma_o, \tau_o)\end{aligned}\tag{4}$$

where: ϵ_o is the octahedral normal strain.

γ_o is the octahedral shear strain.

σ_o is the octahedral normal stress.

τ_o is the octahedral shear stress.

This relationship represents a modified Von Mises theory of yielding. The data obtained from triaxial tests were expressed in

the form of equations [4] by plotting $\tau_o/(\sigma_o)_i$ vs. γ_o . This relationship was then used to obtain pseudoelastic constants during the finite element analysis.

Perumpral *et al.* (10) used the finite element method to study the stress distribution and soil deformation beneath a stationary and moving tractive device. The stress-strain relationship used for the non-linear analysis was similar to that developed by Girijavallabhan and Reese (7). However, in this analysis the stress-strain curve was approximated by two straight lines. This relationship was expressed as:

$$\begin{aligned} \tau_o &= G_o (\sigma_o)_i \gamma_o && \text{if: } \gamma_o \leq (\gamma_o)_y \\ \tau_o &= (G_1 + G_2 \gamma_o)(\sigma_o)_i && \text{if: } \gamma_o > (\gamma_o)_y \end{aligned} \quad [5]$$

where: $(\sigma_o)_i$ is the initial octahedral normal stress.

τ_o is the octahedral shear stress.

γ_o is the octahedral shear strain.

$(\gamma_o)_y$ is the octahedral shear strain at yield.

G_o , G_1 , and G_2 are material parameters.

The stationary wheel problem was analyzed by assuming that the elliptic soil-wheel contact area could be replaced by an equivalent circular contact area. The finite element results compared favorably with closed form solutions.

The analysis of the moving tractive device was performed by considering it as a plane strain problem. From the results of the analysis of the moving tractive device, he concluded that the finite element

approach which was developed could be useful, but insufficient experimental data existed to permit a valid comparison of the experimental and analytical results.

Perloff and Pombo (9) used this technique to study the end restraint effects on the stress distribution in a triaxially loaded soil sample. They assumed horizontal and vertical mid planes of symmetry for a cylindrical sample so that analysis was required for only one quarter of the sample. The constitutive relationship assumed was a modified version of the law proposed at Cambridge by Roscoe (11). The tangent shear modulus was expressed as:

$$\begin{aligned}
 G &= \frac{d\tau_o}{d\gamma_o} = G_o + G_1\sigma_o && \text{if: } \tau_o \leq (\tau_o)_y \\
 G &= \frac{d\tau_o}{d\gamma_o} = G_2 && \text{if: } \tau_o > (\tau_o)_y
 \end{aligned}
 \tag{6}$$

$$(\tau_o)_y = c_o + c_1 \sigma_o$$

where: G is the tangent shear modulus.

γ_o is the octahedral shear strain.

τ_o is the octahedral shear stress.

σ_o is the octahedral normal stress.

$(\tau_o)_y$ is the octahedral shear stress at yield.

G_o, G_1, G_2, c_o and c_1 are material parameters.

The sample was axially loaded by incrementally displacing a rigid loading plate. Their results show that the stress distribution in the sample is not uniform and the effects of the end restraints on the

stress distribution depends upon the soil type.

Triaxial Compression Test

The triaxial compression test has been used widely to determine the strength properties of soil. One of the basic assumptions involved with the triaxial test is that only uniform normal stresses are applied along the sample boundaries and that the material is homogeneous and isotropic. As a result of these assumptions the resulting stress distribution within the sample is assumed to be homogeneous thus the stresses at any point in the sample are directly related to the applied boundary loads. The strains in the sample then can be related to the changes in length and radius of the sample.

These simplifications reduce the analysis of triaxial test results to a simple boundary value problem for which a solution is readily available. Perloff and Pombo (9) have shown that these assumptions are erroneous and that the stress distribution within the sample is not uniform. This knowledge indicates that an analytical approach such as the finite element method might be desirable. With such a technique, the boundary loads could be specified as displacements, forces, or a combination of both.

FINITE ELEMENT ANALYSIS

The finite element technique provides a versatile method of analysis which may be used to solve boundary value problems in structural mechanics, fluid flow, heat and mass transfer, and electrical circuit analysis. In this study the finite element method was used to determine how the state of stress affects the volume change in a soil sample.

The finite element analysis of any problem will be valid only if certain conditions are satisfied. These conditions are:

1. The deformation of adjacent elements must be compatible, so that the line between any two adjacent nodes is initially straight and remains straight in its displaced position.
2. The stress and strain components are constant within any element.
3. The internal forces acting in any element must be in equilibrium with the external forces acting on the element nodes.
4. The internal forces and displacements in any element must be related by the physical properties of that element's material.

The basic steps to be followed in the development of a finite element solution are:

1. Idealization of the system.
2. Selection of the appropriate displacement model.
3. Formation of the individual element stiffness matrices.
4. Formation of the system stiffness matrix.

5. Determination of nodal point displacements.
6. Determination of element stresses.

Element Stiffness Matrix

In this study the effect of stress on soil compaction will be studied using a cylindrical soil sample. Since the geometry of the sample and the boundary loads were symmetric about the vertical axis, the finite element analysis of the system could be carried out by considering it as an axi-symmetric system. Therefore, only the derivation of the stiffness matrix for the axi-symmetric element is included in this section. A typical axi-symmetric sample is shown in Figure 1. Since the displacements within the sample are functions of the radial and vertical coordinates only, the sample can be idealized as a two dimensional system. A typical two dimensional idealized system composed of rectangular elements is shown in Figure 2. Note that these elements represent complete rings in the three dimensional sample.

For a single rectangular element (as shown in Figure 3) in the idealized system let the displacement functions within the element be:

$$w(r,z) = \alpha_1 + \alpha_2 r + \alpha_3 z + \alpha_4 rz \quad [7]$$

$$v(r,z) = \alpha_5 + \alpha_6 r + \alpha_7 z + \alpha_8 rz \quad [8]$$

Where: w is the displacement of the point in the radial direction.
 v is the displacement of the point in the vertical
direction.

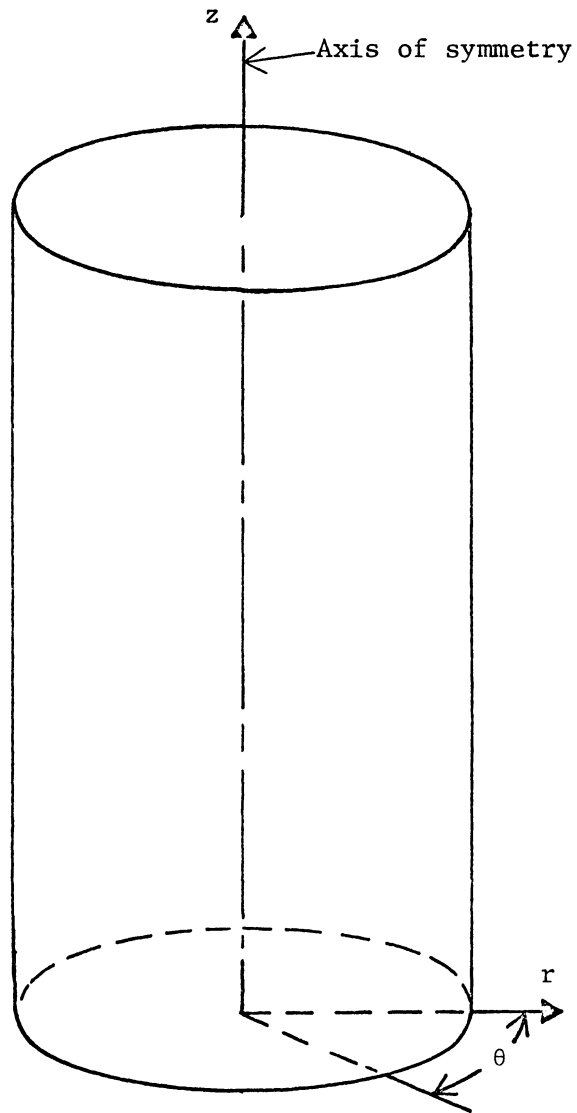


Figure 1. Typical Axi-Symmetric System

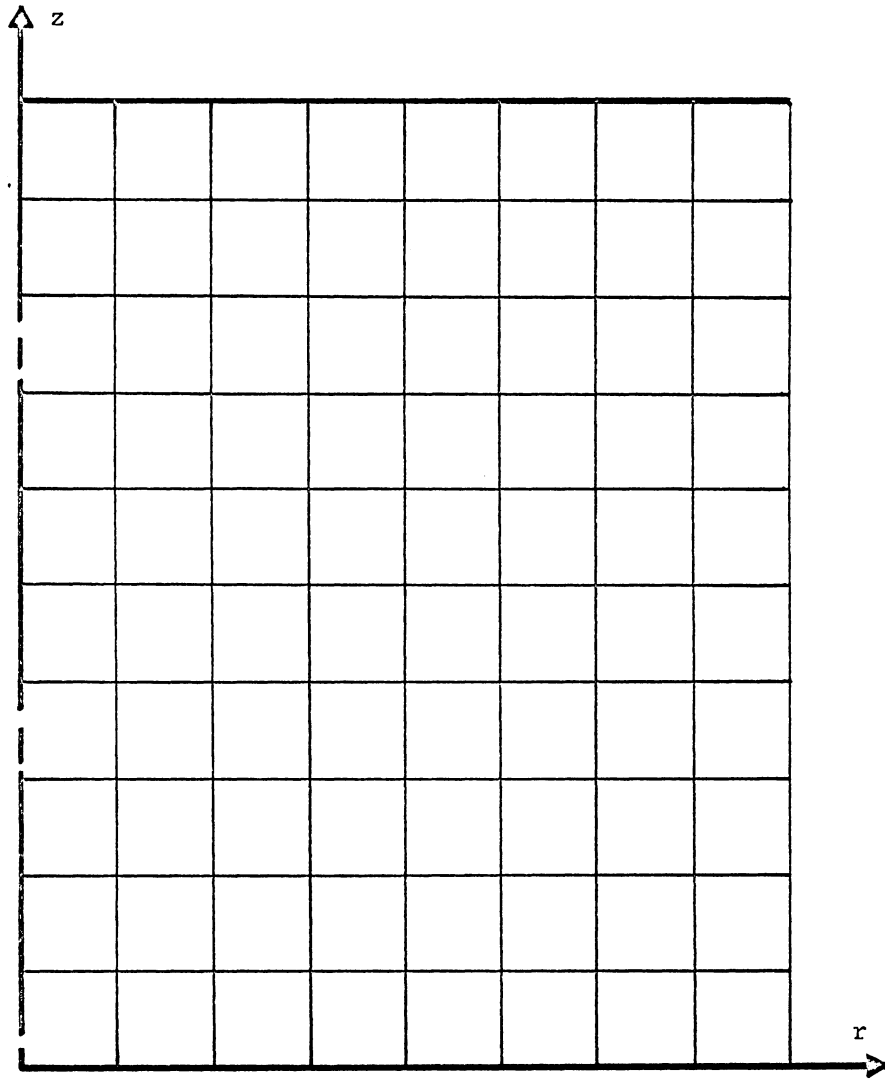


Figure 2. Idealized Two Dimensional System.

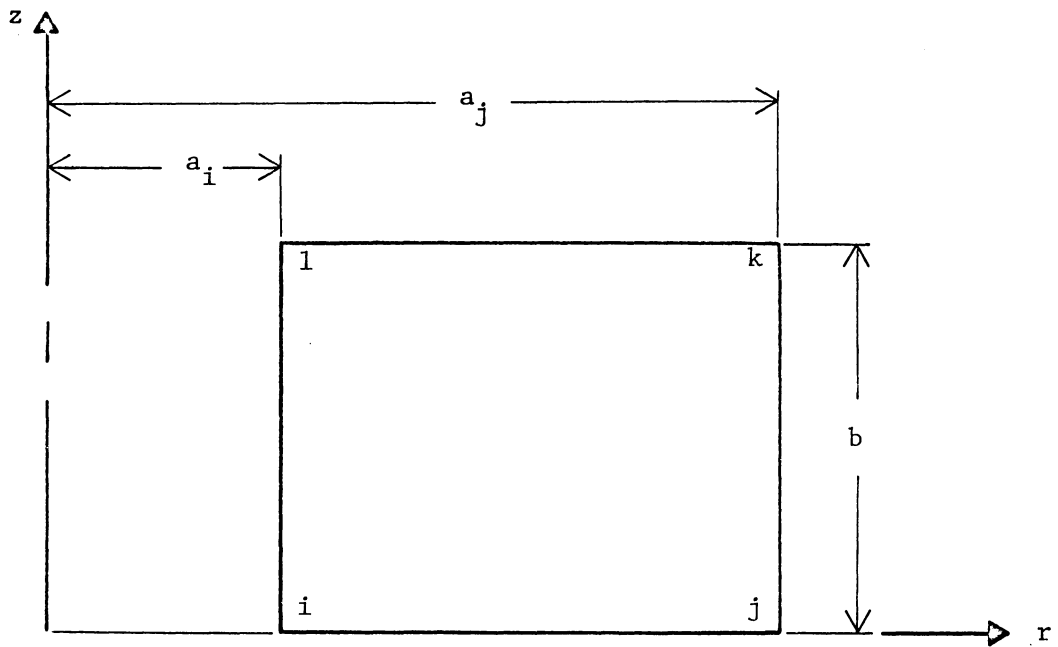


Figure 3. A Typical Rectangular Element in the Idealized System.

r is the radial coordinate of the point.

z is the vertical coordinate of the point.

$\alpha_1 \dots \alpha_6$ are the displacement coefficients.

If this rectangular element, as shown in Figure 3, is acted upon by a force system so that its nodes are displaced as shown in Figure 4, the displacements of each node can be obtained by substituting appropriate nodal point coordinates in equations [7] and [8]. In matrix form the nodal displacements for this element may be expressed as:

$$\begin{Bmatrix} w_i \\ w_j \\ w_k \\ w_l \\ v_i \\ v_j \\ v_k \\ v_l \end{Bmatrix} = \begin{bmatrix} 1 & a_i & 0 & 0 & 0 & 0 & 0 & 0 \\ 1 & a_j & 0 & 0 & 0 & 0 & 0 & 0 \\ 1 & a_j & b & a_j b & 0 & 0 & 0 & 0 \\ 1 & a_i & b & a_i b & 0 & 0 & 0 & 0 \\ 0 & 0 & 0 & 0 & 1 & a_i & 0 & 0 \\ 0 & 0 & 0 & 0 & 1 & a_j & 0 & 0 \\ 0 & 0 & 0 & 0 & 1 & a_j & b & a_j b \\ 0 & 0 & 0 & 0 & 1 & a_i & b & a_i b \end{bmatrix} \begin{Bmatrix} \alpha_1 \\ \alpha_2 \\ \alpha_3 \\ \alpha_4 \\ \alpha_5 \\ \alpha_6 \\ \alpha_7 \\ \alpha_8 \end{Bmatrix} \quad [9]$$

or in matrix notation as:

$$\{u\} = [A] \{\alpha\}. \quad [10]$$

By post multiplying both sides of equation [10] by $[A]^{-1}$, the displacement coefficients are:

$$\{\alpha\} = [A]^{-1} \{u\} \quad [11]$$

From structural mechanics, the strain components at any point within the element can be expressed in terms of the two displacement

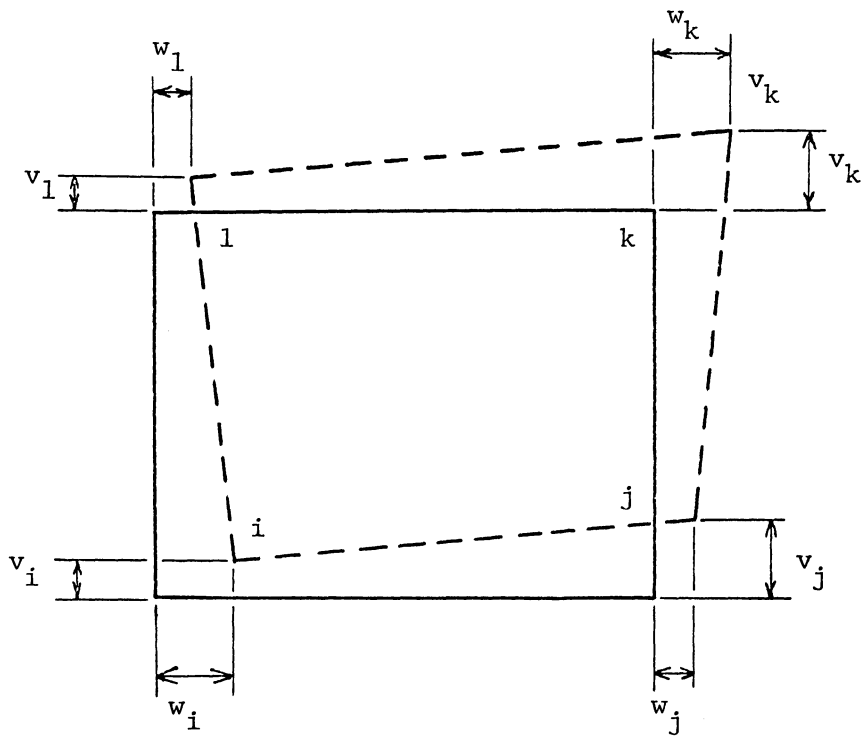


Figure 4. Displaced Rectangular Element.

components as:

$$\left\{ \begin{array}{c} \epsilon_z \\ \epsilon_r \\ \epsilon_\theta \\ \gamma_{rz} \end{array} \right\} = \left\{ \begin{array}{c} \partial v / \partial z \\ \partial w / \partial r \\ w/r \\ \partial v / \partial r + \partial w / \partial z \end{array} \right\} \quad [12]$$

Then by taking appropriate partial derivatives of equations [7] and [8] the strain components can be expressed as:

$$\left\{ \begin{array}{c} \epsilon_z \\ \epsilon_r \\ \epsilon_\theta \\ \gamma_{rz} \end{array} \right\} = \begin{bmatrix} 0 & 0 & 0 & 0 & 0 & 0 & 1 & r \\ 0 & 1 & 0 & z & 0 & 0 & 0 & 0 \\ 1/r & 1 & z/r & z & 0 & 0 & 0 & 0 \\ 0 & 0 & 1 & r & 0 & 1 & 0 & z \end{bmatrix} \{\alpha\} \quad [13]$$

or in matrix notation as:

$$\{\epsilon\} = [H] \{\alpha\} \quad [14]$$

Substituting for $\{\alpha\}$ from equation [11], the strain components may be expressed in terms of the nodal displacements as:

$$\{\epsilon\} = [H] [A]^{-1} \{u\} \quad [15]$$

or by letting:

$$[B] = [H] [A]^{-1} \quad [16]$$

equation [15] becomes:

$$\{\epsilon\} = [B] \{u\} \quad [17]$$

The stresses on a typical element in the continuum are shown in Figure 5. For the axi-symmetric analysis the shear stresses and shear strains in the θ direction are zero. If the material is assumed to be homogeneous, isotropic, and elastic, the stress-strain relationships can be expressed in terms of two elastic constants, E and ν , as:

$$\begin{aligned}
 \epsilon_z &= 1/E (\sigma_z - \nu\sigma_r - \nu\sigma_\theta) \\
 \epsilon_r &= 1/E (-\nu\sigma_z + \sigma_r - \nu\sigma_\theta) \\
 \epsilon_\theta &= 1/E (-\nu\sigma_z - \nu\sigma_r + \sigma_\theta) \\
 \gamma_{rz} &= 2/E (1 + \nu)\tau_{rz}
 \end{aligned}
 \tag{18}$$

Where: E is the modulus of elasticity.

ν is poisson's ratio

ϵ_z , ϵ_r , and ϵ_θ are normal strains in the z , r , and θ directions.

σ_z , σ_r , and σ_θ are normal stresses in the z , r , and θ directions.

γ_{rz} and τ_{rz} are the shear strain and the shear stress acting on the element.

By defining:

$$[C] = \frac{1}{E} \begin{bmatrix} 1 & -\nu & -\nu & 0 \\ -\nu & 1 & -\nu & 0 \\ -\nu & -\nu & 1 & 0 \\ 0 & 0 & 0 & 2(1+\nu) \end{bmatrix}
 \tag{19}$$

equation [18] may be expressed in matrix form as

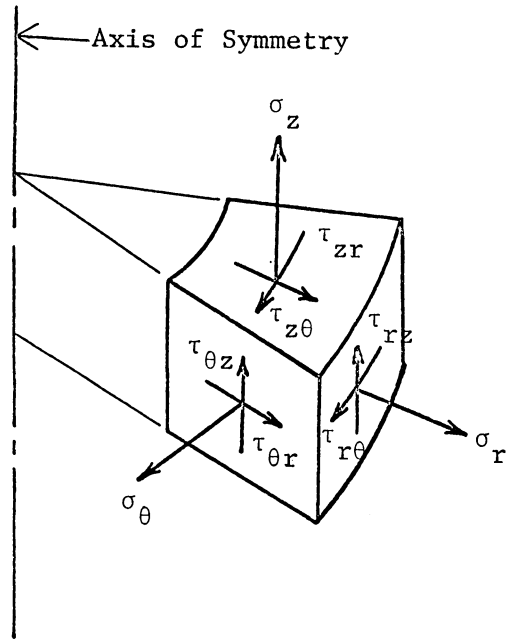


Figure 5. Stresses on an Axi-Symmetric Element.

$$\{\epsilon\} = [C] \{\sigma\} \quad [20]$$

The element stresses may be expressed in terms of the strain components as:

$$\{\sigma\} = [C]^{-1} \{\epsilon\} \quad [21]$$

or by letting:

$$[D] = [C]^{-1} \quad [22]$$

equation [15] becomes:

$$\{\sigma\} = [D] \{\epsilon\} \quad [23]$$

Substituting for the element strains from equation [17], the stresses may be expressed in terms of the nodal displacements as:

$$\{\sigma\} = [D] [B] \{u\} \quad [24]$$

Consider a typical element in the idealized system under the action of a group of forces such that:

$\{f\}$ is the group of nodal forces.

$\{u\}$ is the group of nodal displacements.

$\{\epsilon\}$ is the group of element strains.

$\{\sigma\}$ is the group of element stresses.

If this element's nodes are given a system of virtual displacements, $\{u^*\}$, causing internal strains, $\{\epsilon^*\}$, then the internal and external work performed may be expressed as:

$$\begin{aligned}
 W_{\text{EXT}} &= \{u^*\}^T \{f\} \\
 W_{\text{INT}} &= \int_V \{\epsilon^*\}^T \{\sigma\} dv
 \end{aligned}
 \tag{25}$$

Equating the external and internal work:

$$\{u^*\}^T \{f\} = \int_V \{\epsilon^*\}^T \{\sigma\} dv
 \tag{26}$$

Substituting from equations [17] and [24] for the stresses and strains, and removing the displacements from the integral:

$$\{u^*\}^T \{f\} = \{u^*\}^T \int_V ([B]^T [D] [B] dv) \{u\}
 \tag{27}$$

By taking each element, in the virtual displacement matrix, in succession as unity while the rest are zero, the group of equations each of the form of equation [27] may be written in matrix notation as:

$$[I] \{f\} = [I] \int_V ([B]^T [D] [B] dv) \{u\}
 \tag{28}$$

Since $[I]$ represents the identity matrix, equation [28] may be written as:

$$\{f\} = \int_V ([B]^T [D] [B] dv) \{u\}
 \tag{29}$$

The element stiffness matrix which relates the nodal forces in terms of the displacements is then defined as

$$[k] = \int_V [B]^T [D] [B] dv
 \tag{30}$$

and equation [29] may be written as

$$\{f\} = [k] \{u\}
 \tag{31}$$

System Stiffness Matrix

Based upon the element assemblage information, that is the identification of nodes common to adjacent elements and the nodal boundary conditions, the element stiffness matrices may be combined to form the system stiffness matrix, $[K]$. This stiffness matrix is then used to relate node forces and node displacements for the entire system as:

$$\{F\} = [K] \{U\} \quad [32]$$

Where: $\{F\}$ is the system force matrix.

$\{U\}$ is the system displacement matrix.

$[K]$ is the system stiffness matrix.

Although quite simple in appearance, equation [32] may actually represent several hundred algebraic equations of the form:

$$F_{ir} = K_{ir} U_{ir} + K_{iz} U_{iz} + K_{jr} U_{jr} \dots\dots + K_{nr} U_{nr} \quad [33]$$

for which a simultaneous solution is desired. Before an actual solution is obtained, these equations are divided into three categories, in which:

1. known forces are related to known or unknown displacements.
2. known displacements are related to known or unknown forces.
3. unknown forces are related to unknown displacements.

The first group of equations is solved to determine unknown displacements. The second group is solved to determine unknown forces. Now that some of the unknown forces and displacements have been determined, the third group of equations is subdivided into two groups as 1 and

2 previously and solved as before. When all node displacements have been determined, the element displacement matrices can be formed and the element strains and stresses determined from equations [17] and [24].

METHOD OF ANALYSIS

The Soil Sample

The finite element analysis was carried out on a sample which was two inches in diameter and four inches high. Due to symmetry about the vertical and horizontal axes only one quarter of the sample had to be analyzed. The quarter sample with a cross sectional area of 2 in. x 1 in. was then idealized with square elements. The area of each element was 2.5×10^{-3} in.². The idealized system had 20 elements in each row and a total of 40 rows. There were a total of 800 elements and 861 nodal points.

The section analyzed represented the upper, right quarter of the sample. The top and left boundary nodes were restrained from moving in the radial direction. The lower boundary nodes were restrained from moving in the vertical direction. All other nodes were free to displace in either direction.

Stress-Strain Relationship

It is known that the stress-strain relationship for soil is non-linear in nature. However, from a review of the literature it was found that a majority of the soil mechanics problems solved using analytical methods were based on the assumption that soil is a linearly elastic material. Those who have attempted to include the non-linear behavior in their analysis have used different stress-strain relationships. The relationship used in this study was similar to that used

by Girijavallabhan and Reese (7) as shown in equation [4] in which a generalized Von Mises yield criterion was assumed.

For the finite element analysis, the stress-strain relationship obtained from triaxial tests was modified by plotting $\tau_o/(\sigma_o)_i$ vs. γ_o so that it will be in the form proposed by Girijavallabhan and Reese (7).

where: γ_o is the octahedral shear strain.

τ_o is the octahedral shear stress.

$(\sigma_o)_i$ is the initial octahedral normal stress (confining pressure).

The triaxial test data used were collected by Perumpral *et al.* (10) using prepared soil samples from Ottawa silica sand. Several polynomial equations were fitted to data obtained for various confining pressures. It was found that a third order polynomial approximated the non-linear portion of the stress-strain relationship well with slight deviation in the linear region. Therefore, the modified relationship was approximated in two parts as shown in Figure 6. The linear portion is shown with a broken line, while the non-linear cubic approximation is represented by a solid line. The correlation index (r) for this approximation, as given below, was 0.985.

$$\gamma_o = 0.04641 (\tau_o)_n \quad \text{if: } (\tau_o)_n < (\tau_o)_y \quad [34]$$

$$\gamma_o = 0.01409 (\tau_o)_n - 0.04169 (\tau_o)_n^2 + 0.04558 (\tau_o)_n^3$$

$$\quad \text{if: } (\tau_o)_n \geq (\tau_o)_y \quad [35]$$

where: γ_o is the octahedral shear strain.

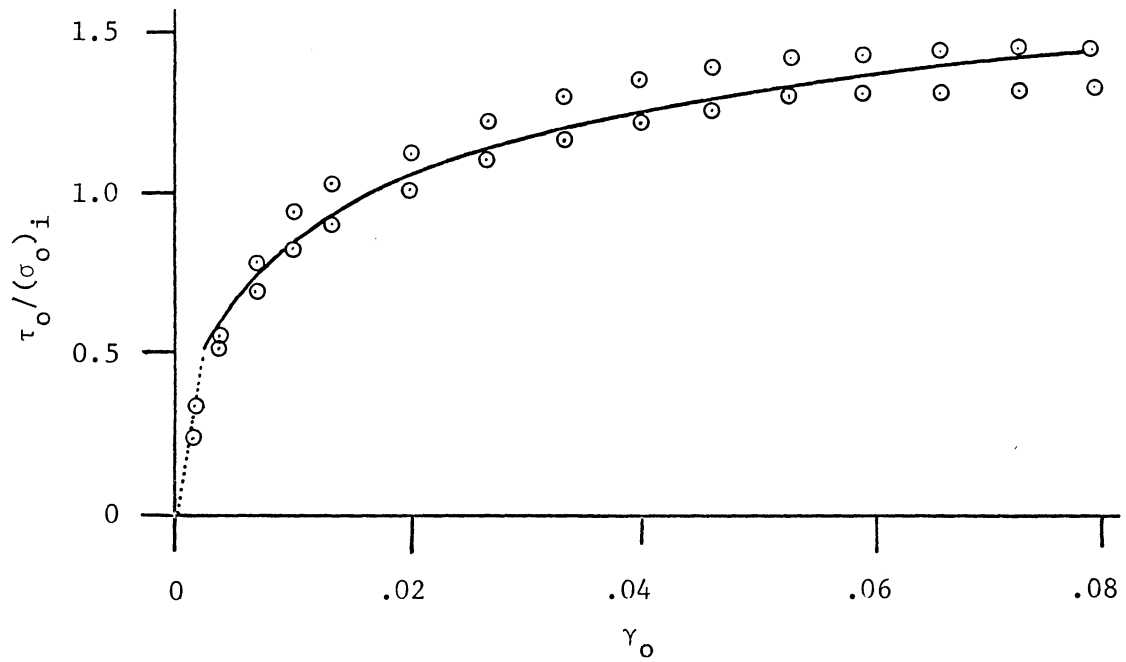


Figure 6. Stress-Strain Relationship used for Finite Element Analysis.

$(\tau_o)_n$ is the normalized octahedral shear
stress = $\tau_o / (\sigma_o)_i$.

τ_o is the octahedral shear stress.

$(\sigma_o)_i$ is the initial octahedral normal stress
(confining pressure).

$(\tau_o)_y$ is the normalized octahedral shear stress at yield.

Non-Linear Analysis

In applying the finite element technique to the analysis on non-linear material response, two general methods may be used, the iterative or the incremental approach. With the iterative method an initial elastic constant is assumed for each element in the idealized system. The total load is applied to the system and the state of stress and strain for each element is determined by the finite element method. Based upon the state of strain, each element's pseudoelastic constants are computed as the secant modulus from the stress-strain relationship. Again a finite element solution is obtained and new values of the elastic constants determined. This iterative procedure is continued until the state of strain for each element reaches equilibrium.

In using the incremental loading technique, an initial elastic constant is determined for each element in the system based upon the initial slope of the stress-strain curve. An increment of the total load is applied to the system and the state of stress and strain is determined for each element by the finite element method. Based upon

the state of stress, each element's elastic modulus is computed as the tangent modulus or slope of the stress-strain curve. This tangent modulus is used as the elastic constant for the next increment of load. This incremental procedure is continued until the total load has been applied to the system.

Both methods have been previously used for finite element analyses of non-linear soil mechanics problems. During this study the incremental loading technique was used to include the non-linear behavior of the soil since this approach could provide information on the force compaction relationship at different stages depending upon the magnitude of the increment chosen.

The analysis was initiated based on the assumption that the sample was 2 inches in diameter and 4 inches long with an initial confining pressure acting on the boundaries. The state of stress at the centroid of each element was initialized to the confining pressure. This state of stress was then used for the computation of the initial modulus of elasticity for each element. A 1 psi increment of axial pressure was then applied to the sample and the corresponding finite element solution was obtained. At the end of each increment, depending upon the state of stress, each element's elastic constants were computed as the tangent modulus of the stress-strain curve. From equations [34] and [35] the tangent shear modulus was determined as:

$$G_1 = \frac{d\tau_o}{d\gamma_o} = 215.5 (\sigma_o)_i \quad [36]$$

$$G_2 = \frac{d\tau_o}{d\gamma_o} = (\sigma_o)_i^3 / \{0.01409 (\sigma_o)_i^2 - 0.08338 (\sigma_o)_i \tau_o + 0.13674 \tau_o^2\} \quad [37]$$

The modulus of elasticity may then be expressed in terms of the shear modulus and poisson's ratio as:

$$E = 2 G(1 + \nu) \quad [38]$$

It was beyond the scope of this study to consider poisson's ratio to be variable. Previous research (7) indicates that variations in ν are small and error associated with the assumption of a constant ν is, likewise, small. Poisson's ratio was assumed to be constant with a value of 0.4.

This elastic modulus was then used for the next increment of axial load. The axial loading was continued until the total axial pressure had reached a predetermined limit (42 psi was used) or until the normalized deviatoric pressure exceeded 3.2. This latter condition corresponded approximately to the shear failure condition in the triaxial tests.

Volumetric Strain

The original volume of a given element may be computed as:

$$v_m = \Delta_m (\bar{r}_m) d\theta \quad [39]$$

Where: v_m is the volume of an element m .

Δ_m is the area of the element cross section.

\bar{r}_m is the radial coordinate of the element centroid.

$d\theta$ is the angular dimension of the sample wedge.

After the application of a set of loads, the modified element volume, v_m^* , may be computed by substituting the appropriate quantities into equation [39]. The average volumetric strain for a typical element, m ,

may then be expressed as

$$s_m = \frac{v_m - v_m^*}{v_m} \quad [40]$$

The total sample volume, before and after loading, may be expressed as the sum of the volumes of all of the elements in the sample, before and after loading.

$$S = \frac{\sum v - \sum v^*}{\sum v} \quad [41]$$

Finite Element Program

The finite element method was employed to compute stresses, volumetric strain and deformation of sand in a triaxial compression test. The program (see Appendix 1) used in this study was developed by Wilson (15) and modified by Perumpral (10) for use in soil sample simulation. For this study, the program was further modified to include the polynomial stress-strain relationship and the method of non-linear analysis presented in previous sections.

RESULTS AND DISCUSSION

The finite element analysis was conducted for confining pressures ranging from 2 to 18 psi intervals. For each confining pressure, the axial pressure was incremented, in 1 psi intervals, from the confining pressure to 42 psi or until the normalized deviatoric pressure reached the point at which the actual soil sample failed in shear. Even though the 42 psi limit was specified within the program, it was found, later, that results of the problems could not be obtained within reasonable time. Such long delays could be avoided either by specifying a higher priority or by specifying a limit on the computation time. Since the use of a higher priority was not economically feasible, a time limit of 120 minutes was placed on the programs. Within this time useable data could be obtained. A better turnaround time could also be obtained by decreasing the number of elements (i.e., increasing the element size) or by increasing the increment of axial pressure. However, either of these procedures would reduce the accuracy of the solution and hence was not used.

For each increment of axial pressure the nodal displacements, element stresses, sample volume, and cross sectional area were computed. The printed output at the end of each increment included:

1. nodal displacements and coordinates.
2. total element stresses, including principal stresses.
3. elastic constants for the elements.
4. volume, area, and volumetric strain for each element.
5. boundary pressure conditions.

6. sample volume, area, and volumetric strain.

Appendix II contains a sample of the printed output for a limited number of nodal points and elements.

Axial Strain in the Sample

To determine the reliability of the finite element solution, and thus the feasibility of using such a method for the soil compaction study, the stress-strain relationships determined from the finite element results were compared with the stress-strain relationship used for the analysis as shown in Figure 7. The relationship shown for both cases are in terms of normalized deviatoric stress and axial strain for various confining pressures.

For each unique confining pressure, the path shown represents that followed in the finite element solution. As the axial pressure increased, each path moved further away from the stress-strain relationship used for the analysis, indicating the additive effect of the error associated with the piece-wise, linear approximation. As the confining pressure increased, the normalized deviatoric pressure increment corresponding to a 1 psi axial pressure increment decreased and the path of axial pressure incrementing followed more closely the given behavior equations.

The error associated with the tangent modulus method of approximation as used in this study was dependent upon the normalized deviatoric pressure increment. By decreasing this increment the analytical solution would have been improved. However, the error associated with the

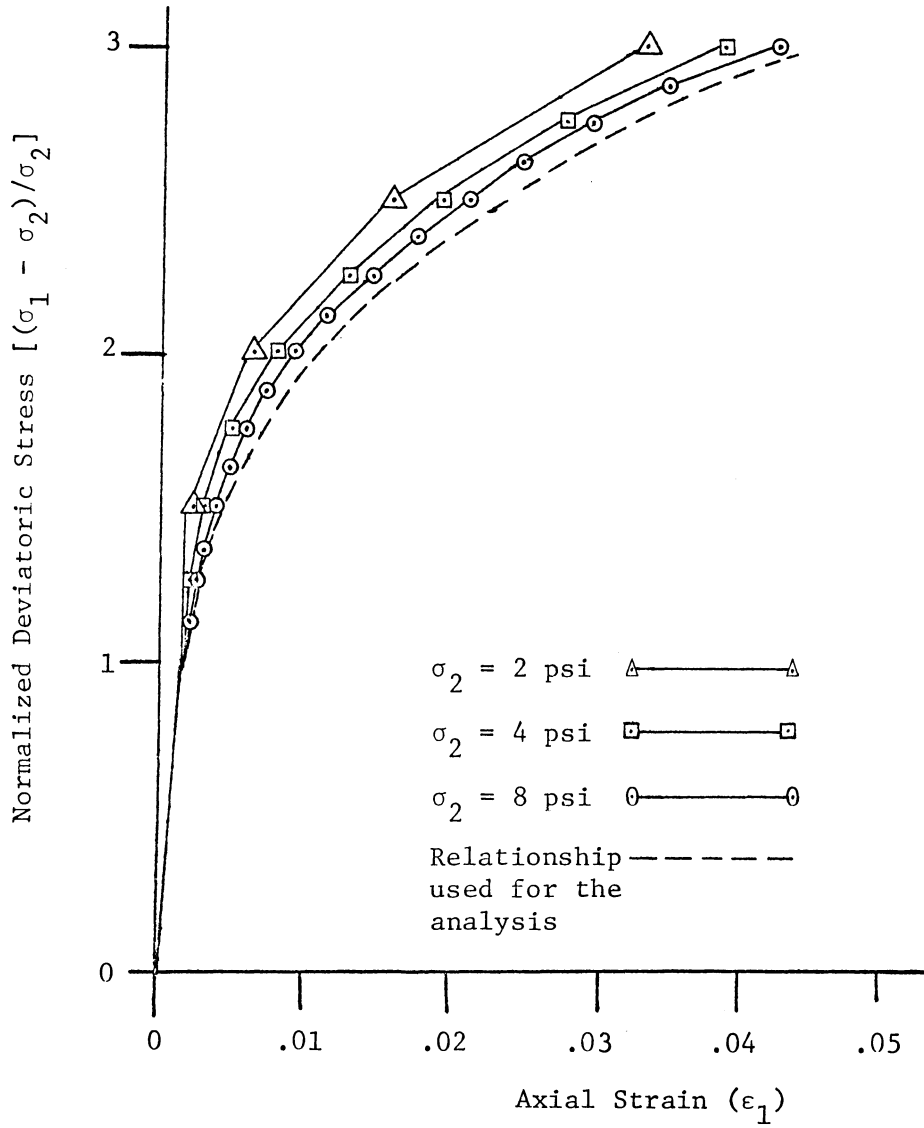


Figure 7. Comparison of Stress-Strain Relationships.

increment used was not deemed significant enough to justify any change in the increment or the method of approximation.

Total Sample Volumetric Strain

In Figure 8 is shown the relationship between the total volumetric strain of the sample and the mean normal stress for various values of maximum shear stress. For a constant maximum shear stress an increase in the mean normal stress produced a decrease in the amount of compaction. This corresponded to an increase in the confining pressure while the difference between the axial and confining pressures remained constant. The increase in confining pressure caused an increase in soil strength resulting in more resistance to deformation and compaction. For higher values of the mean normal stress the amount of compaction exhibited a linear dependence upon the mean normal stress for constant values of maximum shear stress. This behavior corresponded to the linear portion of the stress-strain relationship (see equation [34]) used in the analysis. The range of this linear relationship was determined from the results of the analysis to be:

$$\sigma_m \geq 3.8 \tau_{\max}$$

which corresponded to the linear range used for the analysis.

The relationship between total sample volumetric strain and the maximum shear stress at various levels of mean normal stress is shown in Figure 9. At lower maximum shear stresses the compaction exhibited a linear dependence upon the maximum shear stress for constant values

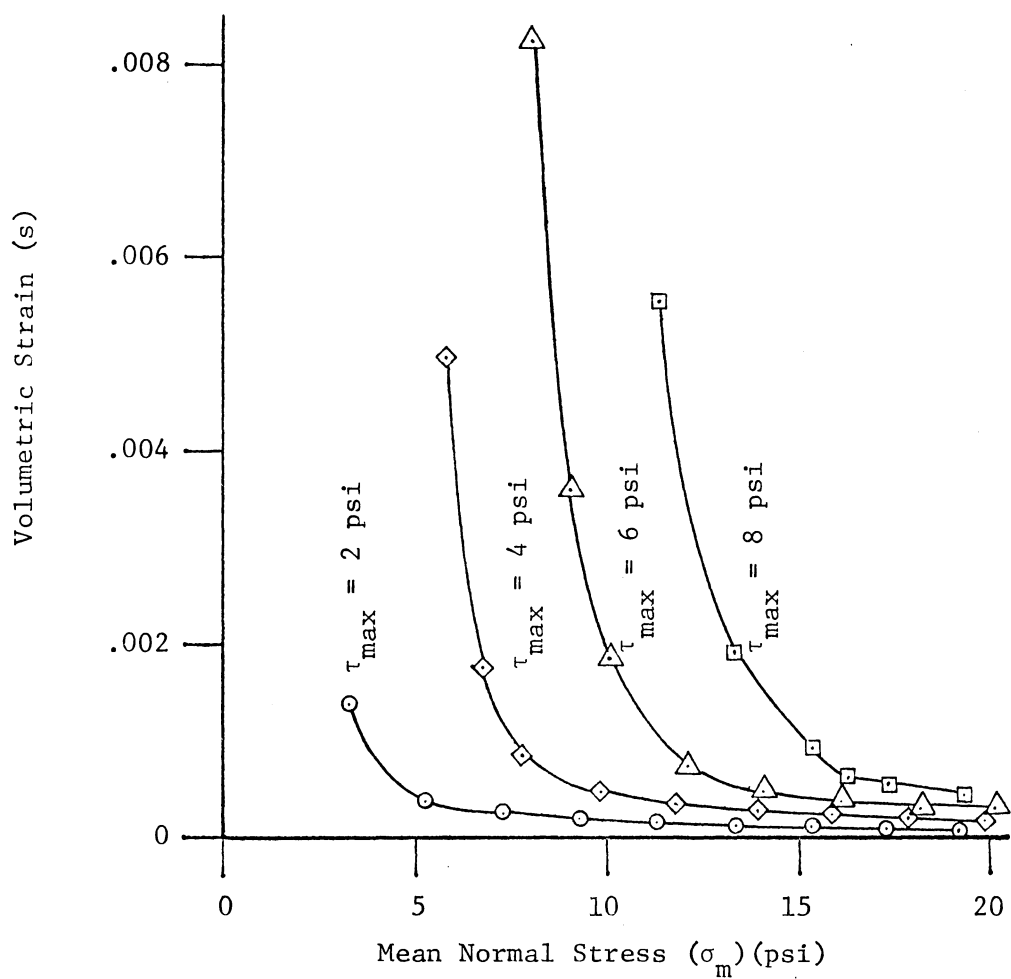


Figure 8. Relationship Between Compaction and Mean Normal Stress.

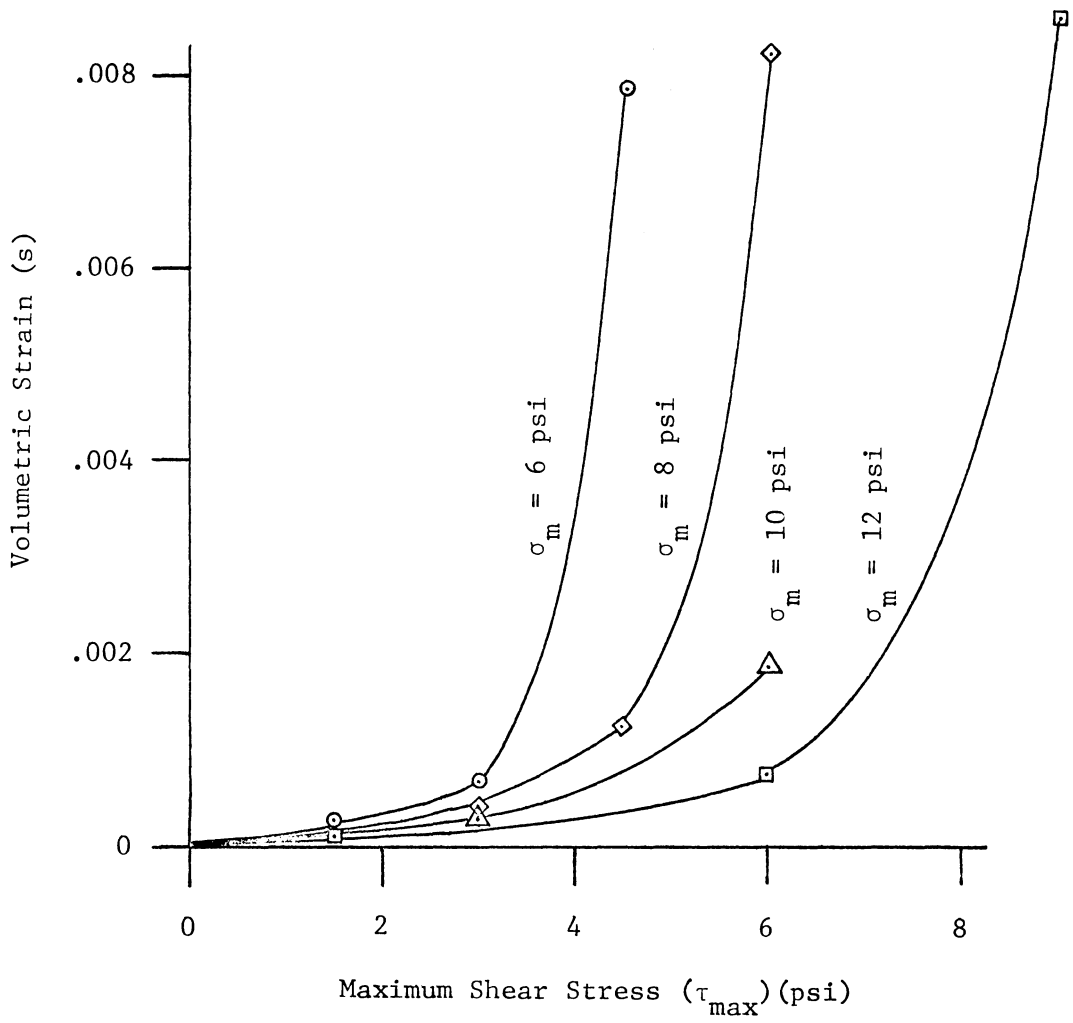


Figure 9. Relationship Between Compaction and Maximum Shear Stress.

of mean normal stress. For constant values of mean normal stress the compaction increases as the maximum shear stress increases. This corresponds to a decrease in the confining pressure and an increase in the axial pressure which results in lower soil strength and more deformation.

The relationship between the mean normal stress and the maximum shear stress for various values of constant volumetric strain is shown in Figure 10. From the relationship shown it is possible to determine which combinations of axial and confining pressures will produce the same amount of compaction.

Based upon the results of the finite element analyses, soil compaction exhibited a dependence upon the maximum shear stress as well as the mean normal stress. In an effort to develop a single relationship which would adequately predict the compaction resulting from both stresses, several empirical equations were fitted to the data obtained from the analyses. The relationship which most suitably predicted the amount of compaction over the entire range of pressure conditions for which data were available was:

$$S = -6.582 \times 10^{-6} \sigma_m + 1.149 \times 10^{-2} \sigma_m \ln [1 + 0.01409 (\tau_{\max})_n - 0.04169 (\tau_{\max})_n^2 + 0.4558 (\tau_{\max})_n^3] \quad [43]$$

where: S is the total volumetric strain.

σ_m is the mean normal stress (psi).

$(\tau_{\max})_n$ is the normalized maximum shear stress
 $= (\sigma_1 - \sigma_2) / (2\sigma_2)$

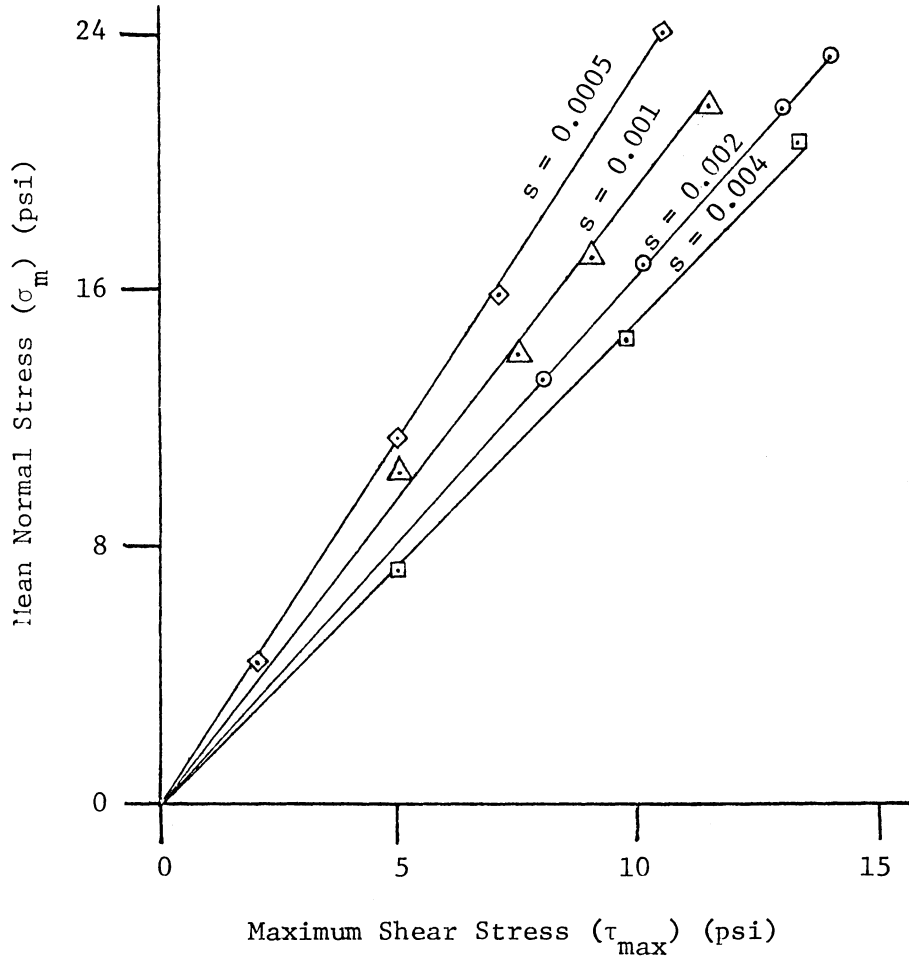


Figure 10. Relationship Between Mean Normal Stress and Maximum Shear Stress for Constant Volumetric Strain.

σ_1 is the axial boundary pressure (psi).

σ_2 is the confining pressure (psi).

The correlation index, r , obtained for this relationship was 0.955.

The total sample volumetric strains as determined from the analyses and from equation [43] for various combinations of axial and confining pressures are shown in Figure 11.

Compaction Zones Within the Sample

Shown in Figure 12 are the compaction zones (contours of equal volumetric strain) for various combinations of axial and confining pressures. For the two cases where the confining pressure was 3 psi and the axial pressures were 9 and 12 psi, maximum compaction occurs on the axis of symmetry in a region slightly below the top of the sample. By looking at the stress distribution within the sample it was found that the mean normal stress was maximum at the top of the sample, but the shear stress was maximum in the region where the maximum compaction occurred. Notice also for 12 psi axial pressure that the lowest volumetric strain occurred at the top of the sample, in the region where the mean normal stress was a maximum. In both of these cases the soil in the regions of maximum compaction exhibited non-linear material response.

For the two cases shown where the confining pressure was 6 psi and the axial pressures were 9 and 12 psi, maximum compaction occurred at the top of the sample on the axis of symmetry. An investigation of the stress distribution within the sample showed that the mean normal was also maximum in the same region. In fact, contours of equal mean

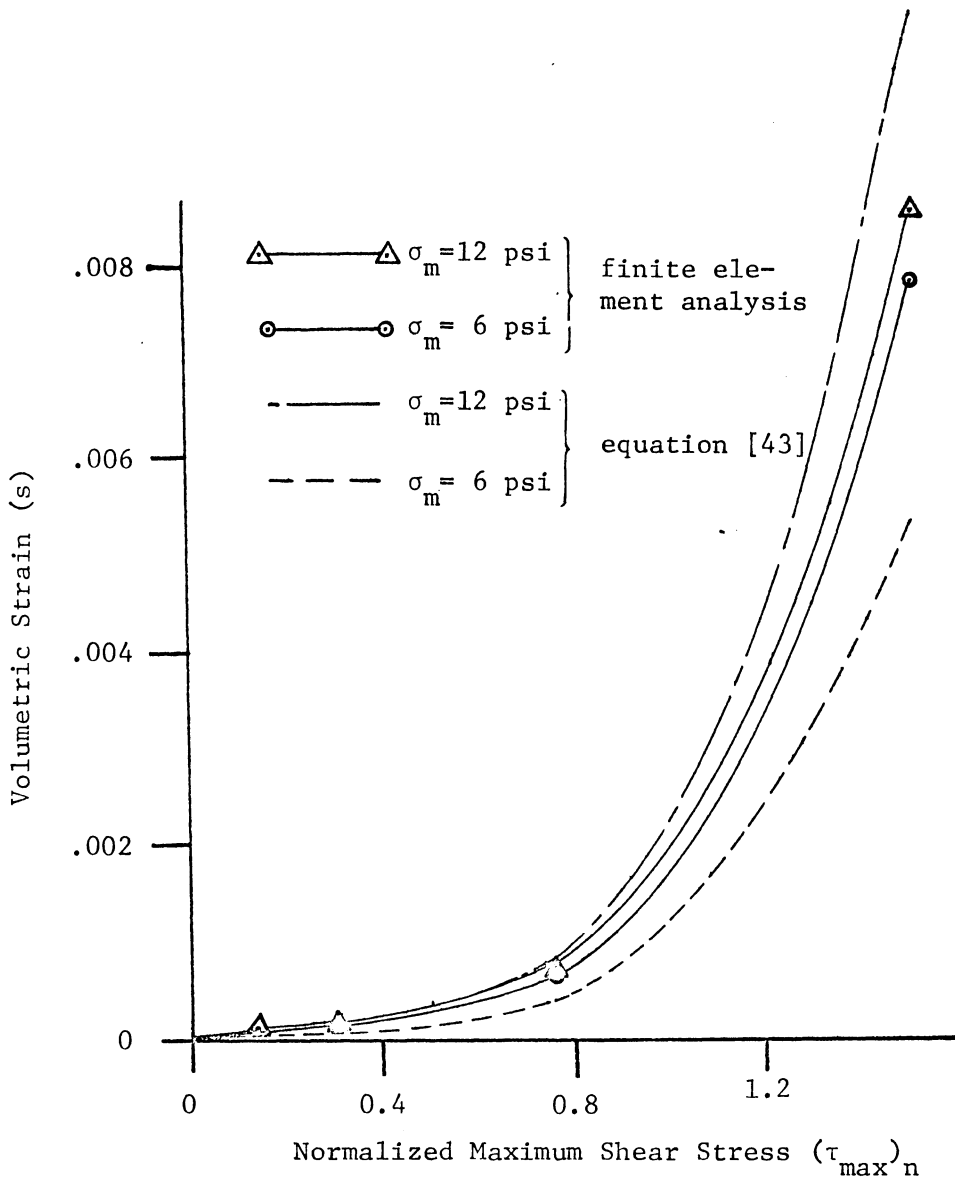


Figure 11. Comparison of Compaction Determined by Finite Element Analysis and the Relationship Developed.

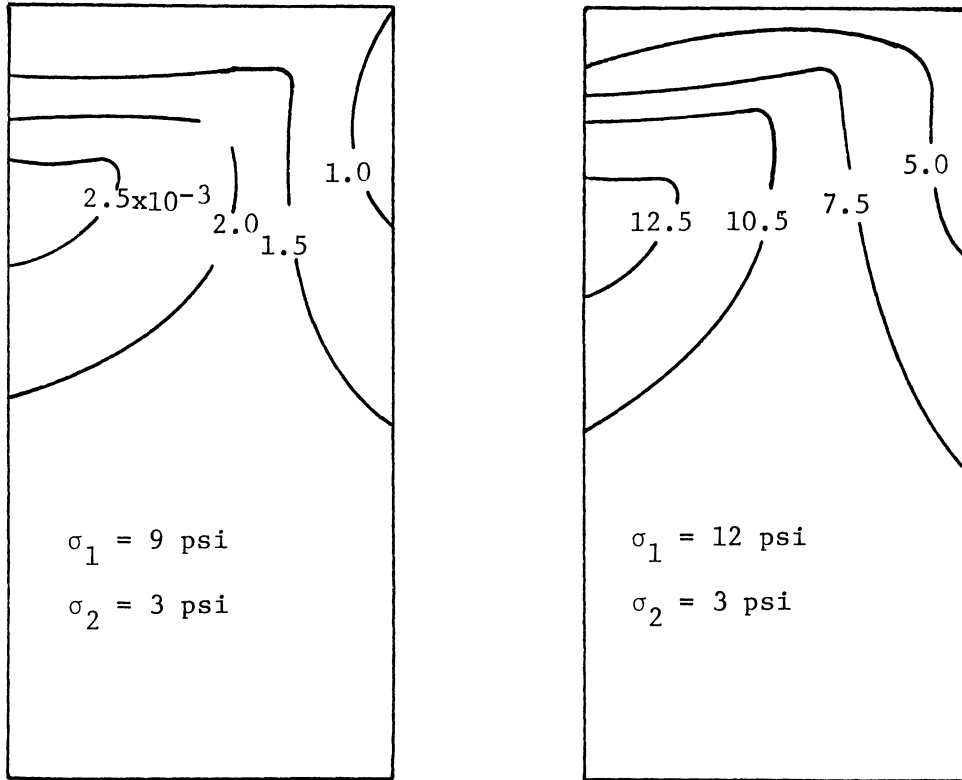


Figure 12a. Volumetric Strain Contours within the Soil Sample.

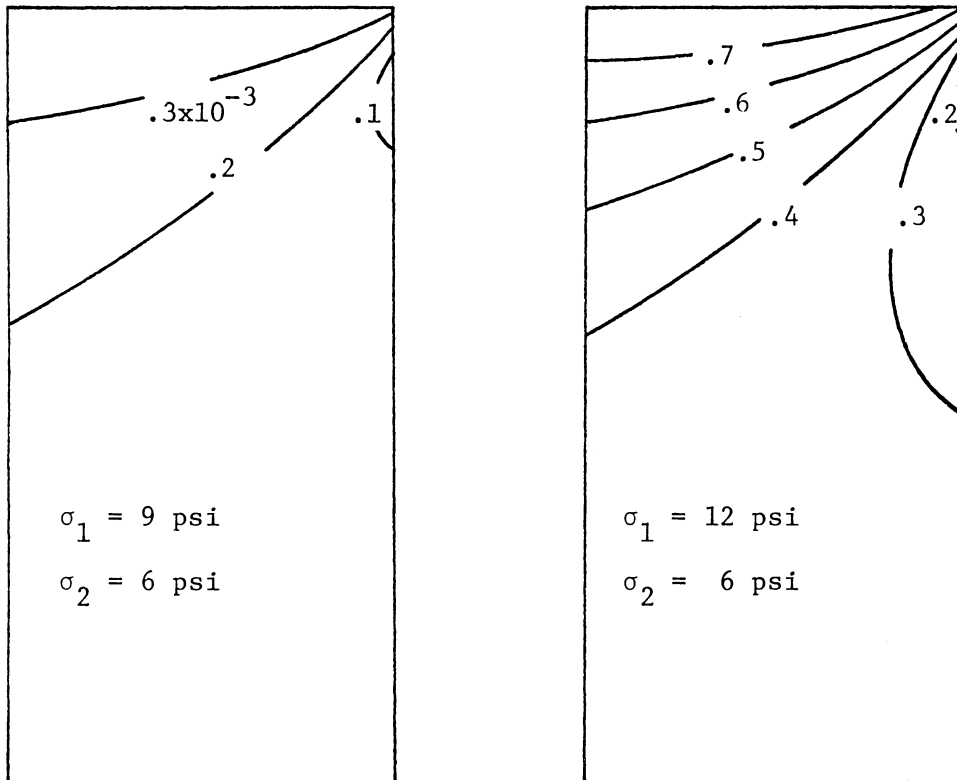


Figure 12b. Volumetric Strain Contours within the Soil Sample.

normal stress could be plotted to nearly coincide with the volumetric strain contours. Further investigation showed that the material response for all elements in the idealized system was still in the elastic range.

The transition of the location of maximum compaction zones from the top of the sample to a region within the sample was observed at several confining pressures as the axial pressure increased. This transition was observed to be occurring when the deviatoric stress exceeded the confining pressure.

CONCLUSIONS

1. The finite element technique can be used to study force-compaction relationships for soils.
2. The amount and variety of information which can be obtained from the finite element solution is far more than that which can be obtained from any experimental tests.
3. Soil compaction is dependent upon the mean normal stress and the maximum shear stress.

RECOMMENDATIONS

The author recommends that further investigations be undertaken to develop suitable stress-strain relationships for soil types other than sand. These relationships could eventually include the creep (time dependent) deformations for soil. As such relationships are developed, analytical methods should be developed in which such relationships could be included.

From the bulk of information obtained by the finite element method, stress-compaction relationships could be studied within a soil sample under given loads. To be of maximum practical usefulness these force-compaction relationships must be extended from the cylindrical sample to larger quantities of soil as it is encountered in the field.

BIBLIOGRAPHY

1. Bailey, A. C. Compaction and shear in compacted soils. Transactions of the ASAE, 14:(2) 201-205, 1971.
2. Bailey, A. C. and Vanden Berg, G. E. Yielding by shear and compaction in unsaturated soils, Transactions of the ASAE, 11:(3) 307-311, 317, 1968.
3. Chancellor, W. J., Schmidt, R. H., and Soehne, W. H. Laboratory measurement of soil compaction and plastic flow, Transactions of the ASAE, 5:(2) 235-239, 1962.
4. Chancellor, W. J. and Schmidt, R. H. Soil deformation beneath surface loads, Transactions of the ASAE, 5:(2) 240-246, 1962.
5. Christian, J. T. Two dimensional analysis of stress and strain in soils, Report No. 3, U. S. Army Engineering Waterways Experiment Station, Vicksburg, Miss., 1966.
6. Dunlap, W. H. and Weber, J. A. Compaction of an unsaturated soil under a general state of stress. Transactions of the ASAE, 14(4) 601-607, 1971.
7. Girijavallabhan, C. V. and Reese, L. C. Finite-element method for problems in soil mechanics, Journal of the Soil Mechanics and Foundations Division, ASCE, 64:(SM2) 473-495, 1968.
8. Harris, W. L., Buchele, W. F., and Malvern, L. E. Relationship of mean stress, volumetric strain and dynamic loads in soil, Transactions of the ASAE, 7:(4) 362-364, 369, 1964.
9. Perloff, W. H. and Pombo, L. E. End restraint effects in the triaxial test, Seventh International Conference of Soil Mechanics and Foundation Engineering, Mexico City, Mexico, 1969.
10. Perumpral, J. V., Liliedahl, J. B., and Perloff, W. H. The finite element method for predicting stress distribution and soil deformation under a tractive device, Transactions of the ASAE, 14:(6) 1184-1188, 1971.
11. Roscoe, K. H. Schofield, A. N., and Wroth, C. P. On yielding of soils, Geotechnique, 8:(1) 22-53, 1958.
12. Soehne, W. H. Fundamentals of pressure distribution and soil compaction under tractor tires, Agricultural Engineer, 39:(5) 276-281, 290, 1958.

13. Vanden Berg, G. E. Buchele, W. F., and Malvern, L. E. Application of continuum mechanics to soil compaction, Transactions of the ASAE, 1:(1) 24-27, 1958.
14. Vanden Berg, G. E. Triaxial measurement of shearing strain and compaction in unsaturated soils, Transactions of the ASAE, 9:(4) 460-463, 467, 1966.
15. Wilson, E. L. Structural analysis of axi-symmetric solids, AIAA Journal, 3:(12), 1965.

APPENDIX I

Finite Element Program

```

      IMPLICIT REAL*8 (A-H,O-Z)
      COMMON ACCELZ,ANGFQ,ANGLF(4),CODE(861),E(1,7,800),VOL,
1          PP(20),Q,R(861),PC(800),TEMP,T(861),UR(861),
2          UZ(861),Z(861),AREA,AREPRT,IRC(20),JRC(20),NP,
3          MTYPE,N,NUMEL,NUMMAT,NUMPC,NUMNP
      COMMON / ARG / C(4,4),D(6,6),DD(3,3),EE(7),F(6,10),
1          H(6,10),HH(6,10),P(10),PR(4),RRR(5),S(10,10),
2          SEG(800,6),SIG(10),TP(6),TT(4),VOLUM(800),
3          XI(10),ZZ(4),ZZZ(5),IX(800,5),LM(4)
      COMMON / BANARG / B(108), A(108,54), MBAND, NUMBLK
      COMMON/PLANE/NPP
      COMMON / PRESUR / PCON,PAXI,PAVE,PDIV,PTAU,PTAUN
      DIMENSION BL(861), BZ(861)
      DIMENSION LFORMT(20),ID(20)
50  READ(5,1111,END=999)ID
      READ(5,1111)LFORMT
      READ(5,LFORMT) NUMNP,NUMEL,NUMMAT,NUMPC,ACELZ,ANGFQ,
1          Q,NP,NPP
      WRITE(6,2000) ID,NUMNP,NUMEL,NUMMAT,NUMPC,ACELZ,ANGFQ,
1          Q, NP
      IF(NPP) 54,56,54
54  WRITE(6,2008)
56  DO 58 M=1,NUMMAT
      PD(M)=0.3
      E(1,1,M)=0.
      E(1,2,M)=2000.0
      E(1,3,M)=.4
      E(1,4,M)=E(1,2,M)
      E(1,5,M)=E(1,3,M)
      F(1,6,M)=0.
      E(1,7,M)=0.0
59  CONTINUE
      NUMTC=1
C    READ AND PRINT OF NODAL POINT DATA
      WRITE(6,2004)
      L=0
      REWIND 3
      READ(5,1111)LFORMT
60  READ(5,LFORMT) N,CODE(N),R(N),Z(N),UR(N),UZ(N),T(N)
      L=L+1
      IF(N-L) 70,100, 80
70  WRITE(6,2009)N
      CALL EXIT
80  DL=N-(L-1)
      DR=(R(N)-R(L-1))/DL
      DZ=(Z(N)-Z(L-1))/DL
      DT=(T(N)-T(L-1))/DL
      NSHORT=N-1
      DO 90 I=L,NSHORT
      R(I)=R(I-1)+DR

```

```

      Z(I)=Z(I-1)+DZ
      T(I)=T(I-1)+DT
      CODE(I)=0.
      UR(I)=0.
  90  UZ(I)=0.
 100  WRITE(6,2002) ( I, CODE(I), R(I), Z(I), UR(I), UZ(I), T(I),
      1      I=L, N)
      DO 110 I=L, N
 110  WRITE(3) I, R(I), Z(I)
      L=N
      IF(N-NUMNIP) 60, 130, 120
 120  WRITE(6,2009) N
      CALL EXIT
 130  CONTINUE
C    READ AND PRINT ELEMENT PROPERTIES
      WRITE(6,2001)
      L=0
      READ(5,1111) LFORMAT
 135  READ(5, LFORMAT) M, ((IX(M, I), I=1, 5), VOLUM(M)
      L=L+1
      IF(M-L) 140, 155, 145
 140  CALL EXIT
 145  MSHORT=M-L
      DI=M-L+1
      DV=(VOLUM(M)-VOLUM(L-1))/DI
      DO 150 I=L, MSHORT
      VOLUM(I)=VOLUM(I-1)+DV
      IX(I, 5)=I
      DO 150 J=1, 4
 150  IX(I, J)=IX(I-1, J)+1
 155  WRITE(6,2003) (I, (IX(I, J), J=1, 5), VOLUM(I), I=L, M)
      L=M
      IF(M-NUMEL) 135, 190, 190
 190  CONTINUE
C    DETERMINE BAND WIDTH
      J=0
      DO 340 N=1, NUMEL
      DO 340 I=1, 4
      DO 325 L=1, 4
      KK=IABS(IX(N, I)-IX(N, L))
      IF (KK-J) 325 , 325 , 320
 320  J=KK
 325  CONTINUE
 340  CONTINUE
      MBAND=2*J+2
C    READ AND PRINT OF PRESSURE BOUNDARY CONDITIONS
      READ(5,1111) LFORMAT
 200  READ(5, LFORMAT) (IBC(I), JBC(I), I=1, NUMPC)
      READ(5,1111) LFORMAT
      READ(5, LFORMAT) PCUN, PCMX, PCDL, PAMX, PABL

```

```

      DO 359 I=1,NUMPC
359 PR(I)=PADL
      PCDN=PCDN-PCDL
392 PCDN=PCDN+PCDL
      IF(PCDN .GT. PCMX)GO TO 50
      REWIND 5
      DO 292 I=1,NUMNP
      BR(I)=0.0
      BZ(I)=0.0
393 READ(3)INP,R(INP),Z(INP)
      DO 294 I=1,NUMEL
      DO 2931 J=1,3
2931 SEG(I,J)=-PCDN
      SEG(I,4)=0.
      E(1,2,I)=431.*(1.+E(1,3,I))*PCDN
      E(1,4,I)=431.*(1.+E(1,5,I))*PCDN
394 CONTINUE
      PAXI=PCDN
398 PAXI=PAXI+PADL
      PDIV=PAXI-PCDN
      DIVIAT=PDIV/PCDN
      PTAU=3.4714045*PDIV
      PTAUN=PTAU/PCDN
      IF(DIVIAT .GT. 3.2)GO TO 292
      IF(PAXI .GT. PAMX)GO TO 292
      PAVF=(PAXI+2.*PCDN)/3.
      WRITE(6,2005)PCDN,PAXI,PAVF
C      FORM STIFFNESS MATRIX
      CALL STIFF
C      SOLVE FOR DISPLACEMENTS
      CALL BANSOL
      DO 360 I=1,NUMNP
      BR(I)=BR(I)+B(2*I-1)
      BZ(I)=BZ(I)+B(2*I)
      R(I)=R(I)+b(2*I-1)
360 Z(I)=Z(I)+B(2*I)
      SUM=0.000
      DO 362 I=1,21
362 SUM=SUM+BZ(I)/2.101
      WRITE(7,3000)PCDN,PAXI,SUM
3000 FORMAT(2F5.1,D20.8)
      WRITE(6,2006)(N,B(2*N-1),B(2*N),R(N),Z(N),BR(N),BZ(N),
1      N=1, NUMNP)
      CALL STRESS
      GO TO 298
999 WRITE(6,2222)
1111 FORMAT(2PA4)
2000 FORMAT(2PA4//
1 28ND NUMBER OF NODAL POINTS----,I3/
2 28NE NUMBER OF ELEMENTS ,I3/

```

```

3 2SHD NUMBER OF DIFF. MATERIALS ,I3/
4 2SHD NUMBER OF PRESSURE CARDS ,I3/
5 2SHD Y-ACCELERATION ,F12.4/
6 2SHD X-ACCELERATION ,F12.4/
7 2SHD REFERENCE TEMPRATURE ,F12.4/
8 2SHD NUMBER OF APPROXIMATIONS ,I3)
2001 FORMAT('I',6X,'EL.',9X,'I',9X,'J',9X,'K',9X,'L',6X,
1 'MTR('//)
2002 FORMAT(I10,F10.0,2F10.2,2F10.3,F10.2)
2003 FORMAT(6I10,F15.3)
2004 FORMAT('I',5X,'NODE',6X,'TYPE',7X,'R',9X,'Z',8X,'UR',
1 8X,'UZ',8X,'TEMP'//)
2005 FORMAT('1CONFINING PRESS. =',F10.2/
1 ' AXIAL PRESS. =',F10.2/
2 ' AVERAGE PRESS. =',F10.2//)
2006 FORMAT(6X,'NODE',6X,'R DISPL',7X,'Z DISPL',7X,
1 ' COORD',7X,'Z COORD',5X,'SUM R DISP',4X,
2 'SUM Z DISP'// (CPI10,DPF14.3,5F14.3))
2008 FORMAT (2SHDPLANE STRAIN STRUCTURE )
2009 FORMAT(2SHD NODAL POINT CARD ERROR N=,I5)
2222 FORMAT('I I HAVE REACHED THE END OF ALL THAT I CAN DO')
STOP
END

```

```

SUBROUTINE STRESS
IMPLICIT REAL*8 (A-H,C-Z)
COMMON ACELZ,ANGFO,ANGLE(4),CODE(861),F(1,7,800),VOL,
1 PF(20),Q,F(861),RD(800),TEMP,T(861),UR(861),
2 UZ(861),Z(861),AREA,AREPRT,IBC(20),JBC(20),NP,
3 MTYPE,N,NUMEL,NUMMAT,NUMPC,NUMNP
COMMON / ARG / C(4,4),D(6,6),DD(3,3),EE(7),F(6,10),
1 H(6,10),HH(6,10),P(10),PR(4),RRR(5),S(10,10),
2 SEC(800,6),SIG(10),TP(6),TT(4),VOLUM(800),
3 XI(10),ZZ(4),ZZZ(5),IX(800,5),LM(4)
COMMON / BANARG / B(108), A(108,54), MBAND, NUMBLK
COMMON/PLANE/NPP
COMMON / PRESUP / PCON,PAXI,PAVE,PDIV,PTAU,PTAUN
C COMPUTE ELEMENT STRESSES
XKF=0.0
XPE=0.0
MPRINT=0
TOTARE=0.
TOTVOL=0.
DO 300 N=1,NUMEL
N=M
IX(N,5)=IABS(IX(N,5))
MTYPE=IX(N,5)

```

```

CALL QUAD
TOTARC=TOTARC+AREA
TOTVCL=TOTVCL+VOL
IX(N,5)=NTYPE
DO 120 I=1,4
  II=2*I
  JJ=2*IX(N,I)
  P(II-1)=B(JJ-1)
120 P(II)=B(JJ)
  DO 150 I=1,2
    RR(I)=P(I+9)
    DO 150 K=1,8
150 RR(I)=RR(I)-S(I+8,K)*P(K)
    COMM=S(9,9)*S(10,10)-S(9,10)*S(10,9)
    IF(COMM) 155,160,155
155 P(9)=(S(10,10)*RR(1)-S(9,10)*RR(2))/COMM
    P(10)=(-S(10,9)*RR(1)+S(9,9)*RR(2))/COMM
160 DO 170 I=1,6
    TP(I)=0.
    DO 170 K=1,10
170 TP(I)=TP(I)+HH(I,K)*P(K)
    RR(1)=TP(2)
    RR(2)=TP(6)
    RR(3)=(TP(1)+TP(2)*RRR(5)+TP(3)*ZZZ(5))/RRR(5)
    RR(4)=TP(3)+TP(5)
176 DO 180 I=1,3
    SIG(I)=-TT(I)
    DO 180 K=1,3
180 SIG(I)=SIG(I)+C(I,K)*RR(K)
    SIG(4)=C(4,4)*RR(4)
C   OUTPUT STRESSES
DO 252 I=1,4
253 SEG(N,I)=SEG(N,I)+SIG(I)
C   CALCULATE PRINCIPAL STRESSES
CC=(SEG(N,1)+SEG(N,2))/2.
BB=(SEG(N,1)-SEG(N,2))/2.
CR=DSQRT(BB*BB+SEG(N,4)**2)
SEG(N,5)=CC+CR
SEG(N,6)=CC-CR
SIGDCT = DABS(SEG(N,1)+SEG(N,2)+SEG(N,3))/3.
TERMA=(SEG(N,1)-SEG(N,2))**2
TERMB=(SEG(N,2)-SEG(N,3))**2
TERMC=(SEG(N,3)-SEG(N,1))**2
TERMD=SEG(N,4)**2
TAUDCT=DSQRT(DABS(TERMA+TERMB+TERMC+ 6.*TERMD))/3.
TON=TAUDCT/PCON
IF(TON - 0.5) 255,256,256
255 CONTINUE
SHEAR=215.5*PCON
GAMDCT=TAUDCT/SHEAR

```

```

      GO TO 257
256 CONTINUE
      COEFA= 0.01409
      COEFB=-0.04169
      COEFC= 0.04558
      GAMDOCT= COEFA*TON +COEFB*TON**2+ COEFC*TON**3
      SHRINV=(COEFA+2.*COEFB*TON+3.*COEFC*TON**2)/PCON
      SHEAR=1. / SHRINV
257 CONTINUE
      E(1,2,N)=2.*SHEAR*(1.+E(1,3,N))
      E(1,4,N)=2.*SHEAR*(1.+E(1,3,N))
      VOLSTR=(VOLUM(N)-VOL)/VOLUM(N)
104 IF(MPRINT) 110,105,110
105 WRITE(6,2000)
      MPRINT=50
110 MPRINT=MPRINT-1
      WRITE(6,2001)N,VOL,AREA,VOLSTR, (SEG(N,I), I=1,8),
1          SIGDOCT,TAUDOCT,TON,GAMDOCT,E(1,2,N),SHEAR
300 CONTINUE
      WRITE(6,2002)TOTVLL, TOTARE
      WRITE(7,3000) PCON,PAXI,PAVE,PDIV,PTAU,PTAUN,TCTVOL,
1          TOTARE
320 RETURN
2000 FORMAT('14L. K(VOLUME AREA DV/VD) SIG R',
1  ' 8X,'SIG Z SIG O TAU R-Z SIG MX SIG MN SIG O ',
3  ' TAU O TAU O N GAM /*100) ET GT/'+'',56X,'-'')
2001 FORMAT(I4,3PF11.7,F9.5,F10.6,3PF8.2,2F8.2,F10.4,3F8.2,
1  ' F7.2,F7.3, 2PF10.5,0PF7.0,F7.0)
2002 FORMAT('1. TOTALS VOLUME AREA' / 8X, 2F11.7)
3000 FORMAT(4F5.1,2F10.5,2F15.8)
      END

```

SUBROUTINE STIFF

IMPLICIT REAL*8 (A-H,C-Z)

```

COMMON ACCLZ,ANGFQ,ANGLE(4),CODE(861),E(1,7,800),VOL,
1      PE(20),Q,R(861),RD(800),TEMP,T(861),UR(861),
2      UZ(861),Z(861),AREA,AREPPT,IBC(20),JBC(20),NP,
3      MTYPE,N,NUMEL,NUMMAT,NUMPC,NUMNP
COMMON / ARG / C(4,4),D(6,6),DD(3,3),EE(7),F(6,10),
1      H(6,10),HH(6,10),P(10),PR(4),RRR(5),S(10,10),
2      SFG(800,6),SIG(10),TP(6),TT(4),VOLUM(800),
3      XI(10),ZZ(4),ZZZ(5),IX(800,5),LM(4)
COMMON / BANARG / B(108), A(108,54), MBAND, NUMELK
COMMON/PLANE/NPP

```

C INITIALIZATION

REWIND 2

NB=27

ND=2*NB

```

ND2=2*ND
STOP=1.0
NUMBLK=0
DO 50 N=1,NL2
  B(N)=1.0
  DO 50 M=1,ND
50  A(N,M)=0.0
C  FORM STIFFNESS MATRIX IN BLOCKS
60  NUMBLK=NUMBLK+1
    NH=NB*(NUMBLK+1)
    NM=NH-NB
    NL=NM-NB+1
    KSHIFT=2*NL-2
    DO 210 N=1,NUMEL
      IF(IX(N,5))210,210,65
65  DO 80 I=1,4
      IF(IX(N,I)-NL)80,70,70
70  IF(IX(N,I)-NM)90,90,80
80  CONTINUE
      GO TO 210
90  CALL QUAD
      IF(VOL)142,142,144
142  WRITE(6,2003) N
      STOP=1.0
144  IF(IX(N,6)-IX(N,4)) 145,165,145
145  DO 150 II=1,9
      CC=S(II,10)/S(10,10)
      P(II)=P(II)-CC*P(10)
      DO 150 JJ=1,9
150  S(II,JJ)=S(II,JJ)-CC*S(10,JJ)
      DO 160 IJ=1,8
      CC=S(II,9)/S(9,9)
      P(II)=P(II)-CC*P(9)
      DO 160 JJ=1,8
160  S(II,JJ)=S(II,JJ)-CC*S(9,JJ)
C  ADD ELEMENT STIFFNESS TO TOTAL STIFFNESS
165  DO 166 I=1,4
166  LM(I)=2+IX(N,I)-2
      DO 200 I=1,4
      DO 200 K=1,2
      II=LM(I)+K-KSHIFT
      KK=2*I-2+K
      B(II)=B(II)+P(KK)
      DO 200 J=1,4
      DO 200 L=1,2
      JJ=LM(J)+L-II+1-KSHIFT
      LL=2*J-2+1
      IF(JJ)200,200,175
175  IF(ND-JJ)180,195,195
180  WRITE(6,2004) N

```

```

        STOP=1.0
        GO TO 210
195  A(II,JJ)=A(II,JJ)+S(KK,LL)
200  CONTINUE
210  CONTINUE
        NITER=1.0
C      ADD CONCENTRATED FORCE WITH IN BLOCK
        DO 250 N=NL,NM
            K=2*N-KSHIFT
            B(K)=B(K)+UZ(N)
250  B(K-1)=B(K-1)+UR(N)
C      BOUNDARY CONDITIONS
C      1. PRESSURE B.C
C      IF(NUMPC) 260,310,260
260  DO 300 L=1,NUMPC
            I=IBC(L)
            J=JBC(L)
            PP=PR(L)/6.0
            DZ=(7(I)-Z(J))*PP
            DR=(R(J)-R(I))*PP
            RX=2.0*R(I)+R(J)
            ZX=R(J)+2.0*R(J)
            IF(NPP) 262,264,262
262  RX=3.0
            ZX=3.0
264  II=2*I-KSHIFT
            JJ=2*J-KSHIFT
            IF(II) 280,280,265
265  IF(II-ND) 270,270,280
270  SINA=0.0
            COSA=1.0
            IF(CODE(I)) 271,272,272
271  SINA = DSIN ( CODE ( I ) )
            COSA = DCOS ( CODE ( I ) )
272  B(II-1)=B(II-1)+RX*(COSA*DZ+SINA*DR)
            B(II)=B(II)-RX*(SINA*DZ-COSA*DR)
280  IF(JJ) 300,300,285
285  IF(JJ-ND) 290,290,300
290  SINA=0.0
            COSA=1.0
            IF(CODE(J)) 291,292,292
291  SINA = DSIN(CODE(J))
            COSA = DCOS(CODE(J))
292  B(JJ-1)=B(JJ-1)+ZX*(COSA*DZ +SINA*DR )
            B(JJ)=B(JJ)-ZX*(SINA*DZ-COSA*DR)
300  CONTINUE
C      2. DISPLACEMENT BOUNDARY CONDITION
310  DO 400 M=NL,NH
            IF (M-NUMMP) 315,315,400
315  U=UR(M)

```

```

      N=2*M-1-KSHIFT
      IF (CODE(N)) 390,401,316
316 IF (CODE(M)-1.) 317,370,317
317 IF (CODE(M)-2.) 318,390,318
318 IF (CODE(M)-3.) 390,380,390
370 CALL MODIFY(A,B,ND2,MBAND,N,U)
      GO TO 407
380 CALL MODIFY(A,B,ND2,MBAND,N,U)
390 U=UZ(M)
      N=N+1
      CALL MODIFY(A,B,ND2,MBAND,N,U)
400 CONTINUE
C   WRITE BLOCK OF EQUATIONS AND SHIFT UP LOWER BLOCK
      WRITE (2) (B(N),(A(N,M),M=1,MBAND),N=1,ND)
      DO 420 N=1,ND
      K=N+ND
      B(N)=B(K)
      B(K)=0.0
      DO 420 M=1,ND
      A(N,M)=A(K,M)
420 A(K,M)=0.0
C   CHECK FOR LAST BLOCK
      IF(NM-NUMNP) 60,480,480
480 CONTINUE
      IF(STOP) 490,500,490
490 CALL EXIT
500 RETURN
2003 FORMAT(26HNEGATIVE AREA ELEMENT NO.,I4)
2004 FORMAT(20HGBAND WIDTH EXCEEDS ALLOWABLE,I4)
      END

```

```

SUBROUTINE QUAD
IMPLICIT REAL*8 (A-H,O-Z)
COMMON ACBLZ,ANGFN,ANGLE(4),CODE(861),E(1,7,800),VOL,
1      PR(20),C,R(861),RO(800),TEMP,T(861),UR(861),
2      UZ(861),Z(861),AREA,AREPRT,IBC(20),JBC(20),NP,
3      MTYPE,N,NUMEL,NUMMAT,NUMPC,NUMNP
COMMON / ARG / C(4,4),D(6,6),DD(3,3),EE(7),F(6,10),
1      H(6,10),HH(6,10),P(10),RR(4),RRR(5),S(10,10),
2      SIG(800,6),SIG(10),TP(6),TT(4),VOLUM(800),
3      XI(10),ZZ(4),ZZZ(5),IX(800,5),LM(4)
COMMON / BANARG / B(108), A(108,54), MBAND, NUMBLK
COMMON/PLANE/NPP
90 T=IX(N,1)
   J=IX(N,2)
   K=IX(N,3)
   L=IX(N,4)
   MTYPE=IX(N,5)

```

```

      IX(N,5)=-IX(N,5)
C      FORM STRESS STRAIN RELATIONSHIP
      TEMP=(T(I)+T(J)+T(K)+T(L))/4.0
104  RATIO=0.0
      DEN=0.0
      M=2
      71 DO 105 KK=1,6
105  EE(KK)=E(M-1, KK+1, MTYPE)
      EE(3)=EE(1)
      EE(4)=EE(2)
      TEMP=TEMP-Q
      IF(NPP) 84,86,85
      84 XX=EE(1)/EE(3)
      COMM=EE(1)/(XX-EE(2)**2)
      C(1,1)=COMM*XX
      C(1,2)=COMM*EE(2)
      C(1,3)=0.0
      C(2,1)=C(1,2)
      C(2,2)=COMM
      C(2,3)=0.0
      C(3,1)=0.0
      C(3,2)=0.0
      C(3,3)=0.0
      C(4,4)=.5*EE(1)/(XX+EE(2))
      GO TO 88
      85 XX=EE(1)/EE(3)
      YY=EE(2)/(XX-EE(2))
      ZX=EE(1)/(1.-EE(2)**2)
      COMM=ZX/(XX-YY**2)
      C(1,1)=COMM*XX
      C(1,2)=COMM*YY
      C(1,3)=0.0
      C(2,1)=0.0
      C(3,2)=0.0
      C(3,3)=0.0
      C(2,1)=COMM*YY
      C(2,2)=COMM
      C(2,3)=0.0
      C(4,4)=.5*ZX/(XX+YY)
      GO TO 88
      86 C(1,1)=1.0/EE(1)
      C(1,2)=-EE(2)/EE(1)
      C(1,3)=-EE(4)/EE(3)
      C(2,1)=C(1,2)
      C(2,2)=C(1,1)
      C(2,3)=C(1,3)
      C(3,1)=C(1,3)
      C(3,2)=C(2,3)
      C(3,3)=1.0/EE(3)
      CALL SYMINV(C,3)

```

```

      C(4,4)=FF(1)/(2.0+2.0*EE(2))
      DO 113 M=1,3
110  TT(M)=((C(N,1)+C(M,2))*EE(5)+C(N,3)*EE(6))*TEMP
C     FORM QUADRILATERAL STIFFNESS MATRIX
      RRR(5)=(R(I)+R(J)+R(K)+R(L))/4.0
      ZZZ(5)=(Z(I)+Z(J)+Z(K)+Z(L))/4.0
      DO 94 M=1,4
      MM=IX(N,M)
      IF(NPP) 93,89,93
      89  IF(R(MM)) 93,91,93
      91  R(MM)=.01*RRR(5)
      IF (CODE(MM)) 93,92,93
      92  CODE(MM)=1.0
      93  PRR(M)=R(MM)
      94  ZZZ(M)=Z(MM)
      DO 100 II=1,10
      P(II)=0.0
      DO 95 JJ=1,6
      95  HH(JJ,II)=0.0
      DO 106 JJ=1,10
100  S(II,JJ)=0.0
      DO 119 II=1,4
      JJ=IX(N,II)
119  ANGLE(II)=CODE(JJ)/57.3
      IF(K-L) 125,120,125
120  CALL TRISTF(1,2,3)
      RRR(5)=(RRR(1)+RRR(2)+RRR(3))/3.0
      ZZZ(5)=(ZZZ(1)+ZZZ(2)+ZZZ(3))/3.0
      VOL=XI(1)
      AREA=AREPRT
      GO TO 139
125  VOL=0.0
      AREA=0.0
      CALL TRISTF(4,1,5)
      VOL=VOL+XI(1)
      AREA=AREA+AREPRT
      CALL TRISTF(1,2,5)
      VOL=VOL+XI(1)
      AREA=AREA+AREPRT
      CALL TRISTF(2,3,5)
      VOL=VOL+XI(1)
      AREA=AREA+AREPRT
      CALL TRISTF(3,4,5)
      VOL=VOL+XI(1)
      AREA=AREA+AREPRT
      DO 140 II=1,6
      DO 140 JJ=1,10
140  HH(II,JJ)=HH(II,JJ)/4.0
139  RETURN
      END

```

```

      SUBROUTINE TRISTF(II,JJ,KK)
      IMPLICIT REAL*8 (A-H,O-Z)
      COMMON ACELZ,ANGFO,ANGLE(4),CODE(861),E(1,7,800),VOL,
1          PR(20),Q,F(861),RD(800),TEMP,T(861),UR(861),
2          OZ(861),Z(861),AREA,AREPRT,IBC(20),JBC(20),NP,
3          MTYPE,N,NUMEL,NUMMAT,NUMPC,NUMNP
      COMMON / ARC / C(4,4),D(6,6),DD(3,2),EE(7),F(6,10),
1          H(6,10),HH(6,10),P(10),RR(4),RRR(5),S(10,10),
2          SEG(800,6),SIG(10),TP(6),TT(4),VOLUM(800),
3          XI(10),ZZ(4),ZZZ(5),IX(800,5),LM(4)
      COMMON / BANARG / B(108), A(108,54), MBAND, NUMBLK
      COMMON/PLANE/NPP
C     1. INITIALIZATION
      LM(1)=II
      LM(2)=JJ
      LM(3)=KK
      PR(1)=R*RR(II)
      RR(2)=R*RR(JJ)
      RR(3)=R*RR(KK)
      RP(4)=R*PR(II)
      ZZ(1)=Z*ZZ(II)
      ZZ(2)=Z*ZZ(JJ)
      ZZ(3)=Z*ZZ(KK)
      ZZ(4)=Z*ZZ(II)
      85 DO 100 I=1,6
         DO 90 J=1,10
            F(I,J)=0.0
      90 H(I,J)=1.0
         DO 100 J=1,6
      100 D(I,J)=1.0
C     5. FORM INTEGRAL(G)T*(C)*(G)
      CALL INTER (XI,RR,ZZ)
      D(2,6)=XI(1)*(C(1,2)+C(2,3))
      D(3,5)=XI(1)*C(4,4)
      D(5,5)=XI(1)*C(4,4)
      D(6,6)=XI(1)*C(2,2)
      IF(NPP) 1,4,106,104
      104 D(2,2)=XI(1)*C(1,1)
         D(3,3)=XI(1)*C(4,4)
         GO TO 103
      106 D(1,1)=XI(2)*C(3,3)
         D(1,2)=XI(2)*(C(1,3)+C(3,3))
         D(1,3)=XI(5)*C(3,3)
         D(1,6)=XI(2)*C(2,3)
         D(2,2)=XI(1)*(C(1,1)+2.0*C(1,3)+C(3,3))
         D(2,3)=XI(4)*(C(1,5)+C(3,3))
         D(3,3)=XI(6)*C(3,3)+XI(1)*C(4,4)

```

```

      D(3,6)=XI(4)*C(2,3)
108 DO 112 I=1,6
      DO 113 J=1,6
110 D(J,I)=D(I,J)
C     4. FORM COEFFICIENT DISPLACEMENT TRANSFORMATION MATRIX
      COMM= KR(2)*(ZZ(3)-ZZ(1))
1      +RR(1)*(ZZ(2)-ZZ(3))
2      +KR(3)*(ZZ(1)-ZZ(2))
      AREPRT=COMM/2.
      DD(1,1)=(PR(2)*ZZ(3)-PR(3)*ZZ(2))/COMM
      DD(1,2)=(PR(3)*ZZ(1)-PR(1)*ZZ(3))/COMM
      DD(1,3)=(RR(1)*ZZ(2)-PR(2)*ZZ(1))/COMM
      DD(2,1)=(ZZ(2)-ZZ(3))/COMM
      DD(2,2)=(ZZ(3)-ZZ(1))/COMM
      DD(2,3)=(ZZ(1)-ZZ(2))/COMM
      DD(3,1)=(RR(3)-RR(2))/COMM
      DD(3,2)=(RR(1)-RR(3))/COMM
      DD(3,3)=(RR(2)-RR(1))/COMM
      DO 123 I=1,3
      J=2+LM(I)-1
      H(1,J)=DD(1,I)
      H(2,J)=DD(2,I)
      H(3,J)=DD(3,I)
      H(4,J+1)=DD(1,I)
      H(5,J+1)=DD(2,I)
123 H(6,J+1)=DD(3,I)
C     ROTATE UNKNOWNNS IF REQUIRED
      DO 125 J=1,2
      I=LM(J)
      IF(ANGLE(I)) 122,125,125
122 SINA = DSIN(ANGLE(I))
      COSA = DCOS(ANGLE(I))
      IJ=2*I
      DO 124 K=1,6
      TEM =H(K,IJ-1)
      H(K,IJ-1)=TEM*COSA+H(K,IJ)*SINA
124 H(K,IJ)=-TEM*SINA+H(K,IJ)*COSA
125 CONTINUE
C     5. FORM ELEMENT STIFFNESS MATRIX (H)T*(D)*(H)
      DO 133 J=1,10
      DO 134 K=1,6
      IF (H(K,J)) 128,130,128
128 DO 129 I=1,6
129 F(I,J)=F(I,J)+D(I,K)*H(K,J)
130 CONTINUE
      DO 143 I=1,10
      DO 144 K=1,6
      IF (H(K,I))138,140,138
138 DO 139 J=1,10
139 S(I,J)=S(I,J)+H(K,I)*F(K,J)

```

```

140 CONTINUE
C   6. FORM THERMAL LOAD MATRIX
   IF(NPP) 145,150,145
145 TT(3)=0.0
   COMM=XI(1)*FE(4)
150 COMM=RO(MTYPT)*ANGFC**2
   TP(1)=COMM*XI(7)+XI(2)*TT(3)
   TP(2)=COMM*XI(9)+XI(1)*(TT(1)+TT(3))
   TP(3)=COMM*XI(10)+XI(4)*TT(3)
   COMM=-RO(MTYPT)*ACFLZ
   TP(4)=COMM*XI(1)
   TP(5)=COMM*XI(7)
   TP(6)=COMM*XI(8)+XI(1)*TT(2)
   DO 160 I=1,10
   DO 160 K=1,6
160 P(I)=P(I)+H (K,I)*TP(K)
C   FORM STRAIN TRANSFORMATION MATRIX
400 DO 410 I=1,6
   DO 410 J=1,10
410 HH(I,J)=HH(I,J)+H(I,J)
   RETURN
   END

```

```

SUBROUTINE MODIFY(A,B,NEQ,MBAND,N,U)
IMPLICIT REAL*8 (A-H,O-Z)
DIMENSION A(108,54) ,B(108)
DO 250 M=2,MBAND
K=N-M+1
IF(K) 235,235,230
230 B(K)=B(K)-A(K,M)*U
   A(K,M)=0.0
235 K=N+M-1
IF(NEQ-K) 250,240,240
240 B(K)=B(K)-A(N,M)*U
   A(N,M)=0.0
250 CONTINUE
   A(N,1)=1.0
   B(N)=U
   RETURN
   END

```

```

SUBROUTINE BANSOL
IMPLICIT REAL*8 (A-H,O-Z)
COMMON / BANARG / B(108) , A(108,54) , MM ,      NUMBLK
NN=54
NL=NN+1

```

```

      NH=NN+NN
      REWIND 1
      REWIND 2
      NB=0
      GO TO 150
C     REDUCE EQUATIONS BY BLOCKS
C     1. SHIFT BLOCK OF EQUATIONS
100  NB=NB+1
      DO 125 N=1,NN
      NM=NN+N
      B(N)=B(NM)
      B(NM)=0.0
      DO 125 M=1,MM
      A(N,M)=A(NM,M)
125  A(NM,M)=0.0
C     2. READ NEXT BLOCK OF EQUATIONS
      IF(NUMBLK-NB) 150,200,150
150  READ(2) (B(N), (A(N,M),M=1,MM),N=NL,NH)
      IF(NB) 230,130,200
C     3. REDUCE BLOCK OF EQUATION
200  DO 300 N=1,NN
      IF (A(N,1)) 225,300,225
225  B(N)=B(N)/A(N,1)
      DO 275 L=2,MM
      IF(A(N,L)) 230,275,230
230  C=A(N,L)/A(N,1)
      I=N+L-1
      J=0
      DO 250 K=L,MM
      J=J+1
250  A(I,J)=A(I,J)-C*A(N,K)
      B(I)=B(I)-A(N,L)*B(N)
      A(N,L)=C
275  CONTINUE
300  CONTINUE
C     4. WRITE BLOCK OF REDUCED EQUATIONS ON TAPE 2
      IF(NUMBLK-NB) 375,400,375
375  WRITE(1) (B(N), (A(N,M),M=2,MM),N=1,NN)
      GO TO 100
C     BACK SUBSTITUTION
400  DO 450 M=1,NN
      N=NN+1-M
      DO 425 K=2,MM
      L=N+K-1
425  B(N)=B(N)-A(N,K)*B(L)
      NM=N+NN
      B(NM)=B(N)
450  A(NM,NP)=B(N)
      NB=NB-1
      IF(NB) 475,500,475

```

```

475 BACKSPACE 1
   READ(1)(B(N),(A(N,M),M=2,MM),N=1,NN)
   BACKSPACE 1
   GO TO 411
C   ORDER UNKNOWN IN B ARRAY
500 K=1
   DO 600 NB=1,NUMBLK
   DO 600 N=1,NN
   NM=N+NB
   K=K+1
600 B(K)=A(NM,NB)
   RETURN
   END

```

```

SUBROUTINE INTER(XI,RR,ZZ)
IMPLICIT REAL*8 (A-H,O-Z)
DIMENSION FR(4),ZZ(4),XI(10),XM(6),R(6),Z(6),XX(6)
COMMON/PLANE/NPP
DATA XX / 3*1.0D0 , 3*3.0D0 /
COMM= RR(2)*(ZZ(3)-ZZ(1))
1      +RR(1)*(ZZ(2)-ZZ(3))
2      +RR(3)*(ZZ(1)-ZZ(2))
COMM=COMM/24.0
R(1)=RR(1)
R(2)=FR(2)
R(3)=FR(3)
R(4)=(R(1)+R(2))/2.0
R(5)=(R(2)+R(3))/2.0
R(6)=(R(3)+R(1))/2.0
Z(1)=ZZ(1)
Z(2)=ZZ(2)
Z(3)=ZZ(3)
Z(4)=(Z(1)+Z(2))/2.0
Z(5)=(Z(2)+Z(3))/2.0
Z(6)=(Z(3)+Z(1))/2.0
IF (NPP) 10,30,10
10 DO 20 I=1,6
20 XM(I)=XX(I)
   GO TO 40
30 DO 35 I=1,6
35 XM(I)=XX(I)*R(I)
40 DO 50 I=1,10
50 XI(I)=0.0
   DO 100 I=1,6
   XI(1)=XI(1)+XM(I)
   XI(2)=XI(2)+XM(I)/R(I)
   XI(3)=XI(3)+XM(I)/(R(I)**2)
   XI(4)=XI(4)+XM(I)*Z(I)/R(I)

```

```

XI(5)=XI(5)+XM(I)*Z(I)/(R(I)**2)
XI(6)=XI(6)+XM(I)*Z(I)**2/(R(I)**2)
XI(7)=XI(7)+XM(I)*R(I)
XI(8)=XI(8)+XM(I)*Z(I)
XI(9)=XI(9)+XM(I)*R(I)**2
XI(10)=XI(10)+XM(I)*R(I)*Z(I)
100 CONTINUE
DO 150 I=1,10
150 XI(I)=XI(I)*COMM
RETURN
END

```

```

SUBROUTINE SYMINV(A,NMAX)
IMPLICIT REAL*8 (A-H,D-Z)
DIMENSION A(4,4)
DO 200 N=1,NMAX
D=A(N,N)
DO 100 J=1,NMAX
100 A(N,J)=-A(N,J)/D
DO 150 I=1,NMAX
IF(N-I) 110,150,110
110 DO 140 J=1,NMAX
IF (N-J) 120,140,120
120 A(I,J)=A(I,J)+A(I,N)*A(N,J)
140 CONTINUE
150 A(I,N)=A(I,N)/D
A(N,N)=1.0/D
200 CONTINUE
RETURN
END

```

APPENDIX II

Sample Computer Output

CONFINING PRESSURE = 10 PSI
 AXIAL PRESSURE = 25 PSI
 AVERAGE PRESSURE = 15 PSI

NODE	R DISPL.	SUM R DISPL.	R COORD.
1	0.0000-00	0.0000-00	2.5000-04
2	0.0000-00	0.0000-00	5.0000-02
3	0.0000-00	0.0000-00	1.0000-01
4	0.0000-00	0.0000-00	1.5000-01
5	0.0000-00	0.0000-00	2.0000-01
6	0.0000-00	0.0000-00	2.5000-01
7	0.0000-00	0.0000-00	3.0000-01
8	0.0000-00	0.0000-00	3.5000-01
9	0.0000-00	0.0000-00	4.0000-01
10	0.0000-00	0.0000-00	4.5000-01
11	0.0000-00	0.0000-00	5.0000-01
12	0.0000-00	0.0000-00	5.5000-01
13	0.0000-00	0.0000-00	6.0000-01
14	0.0000-00	0.0000-00	6.5000-01
15	0.0000-00	0.0000-00	7.0000-01
16	0.0000-00	0.0000-00	7.5000-01
17	0.0000-00	0.0000-00	8.0000-01
18	0.0000-00	0.0000-00	8.5000-01
19	0.0000-00	0.0000-00	9.0000-01
20	0.0000-00	0.0000-00	9.5000-01
21	0.0000-00	0.0000-00	1.0000-00
22	0.0000-00	0.0000-00	2.5000-04
23	1.1450-06	8.2350-06	5.0010-02
24	2.2910-06	1.6530-05	1.0000-01
25	3.4390-06	2.4920-05	1.5000-01
26	4.5900-06	3.3460-05	2.0000-01
27	5.7560-06	4.2210-05	2.5000-01
28	6.9830-06	5.1280-05	3.0010-01
29	8.3030-06	6.0730-05	3.5010-01
30	9.6800-06	7.0570-05	4.0010-01
31	1.1070-05	8.0830-05	4.5010-01
32	1.2470-05	9.1680-05	5.0010-01
33	1.3930-05	1.0330-04	5.5010-01
34	1.5590-05	1.1600-04	6.0010-01
35	1.7500-05	1.3000-04	6.5010-01
36	1.9460-05	1.4540-04	7.0010-01
37	2.1450-05	1.6280-04	7.5020-01
38	2.3840-05	1.8340-04	8.0020-01
39	2.6910-05	2.0850-04	8.5020-01
40	3.0750-05	2.4080-04	9.0020-01
41	3.5090-05	2.9460-04	9.5030-01

CONFINING PRESSURE = 10 PSI
 AXIAL PRESSURE = 25 PSI
 AVERAGE PRESSURE = 15 PSI

NODE	Z DISPL.	SUM Z DISPL.	Z COORD.
1	-1.3120-03	-7.3510-03	-5.7350-02
2	-1.3120-03	-7.3510-03	-5.7350-02
3	-1.3110-03	-7.3450-03	-5.7340-02
4	-1.3090-03	-7.3360-03	-5.7340-02
5	-1.3060-03	-7.3230-03	-5.7320-02
6	-1.3020-03	-7.3060-03	-5.7310-02
7	-1.2970-03	-7.2850-03	-5.7280-02
8	-1.2910-03	-7.2590-03	-5.7260-02
9	-1.2850-03	-7.2300-03	-5.7230-02
10	-1.2270-03	-7.1950-03	-5.7200-02
11	-1.2690-03	-7.1550-03	-5.7150-02
12	-1.2580-03	-7.1080-03	-5.7110-02
13	-1.2470-03	-7.0550-03	-5.7050-02
14	-1.2340-03	-6.9940-03	-5.6990-02
15	-1.2190-03	-6.9240-03	-5.6920-02
16	-1.2020-03	-6.8430-03	-5.6840-02
17	-1.1830-03	-6.7940-03	-5.6750-02
18	-1.1600-03	-6.6390-03	-5.6640-02
19	-1.1330-03	-6.5050-03	-5.6510-02
20	-1.1010-03	-6.3380-03	-5.6340-02
21	-1.0650-03	-6.0870-03	-5.6090-02
22	-1.3080-03	-7.2870-03	-1.0730-01
23	-1.3070-03	-7.2860-03	-1.0730-01
24	-1.3060-03	-7.2810-03	-1.0730-01
25	-1.3040-03	-7.2710-03	-1.0730-01
26	-1.3010-03	-7.2580-03	-1.0730-01
27	-1.2970-03	-7.2410-03	-1.0720-01
28	-1.2920-03	-7.2200-03	-1.0720-01
29	-1.2870-03	-7.1940-03	-1.0720-01
30	-1.2800-03	-7.1650-03	-1.0720-01
31	-1.2730-03	-7.1300-03	-1.0710-01
32	-1.2640-03	-7.0890-03	-1.0710-01
33	-1.2530-03	-7.0420-03	-1.0700-01
34	-1.2420-03	-6.9880-03	-1.0700-01
35	-1.2290-03	-6.9260-03	-1.0690-01
36	-1.2140-03	-6.8560-03	-1.0690-01
37	-1.1970-03	-6.7740-03	-1.0680-01
38	-1.1770-03	-6.6780-03	-1.0670-01
39	-1.1550-03	-6.5660-03	-1.0660-01
40	-1.1280-03	-6.4290-03	-1.0640-01
41	-1.0950-03	-6.2560-03	-1.0630-01

EL.	(VOL.	AREA	STR)*K	SIG-R	SIG-Z	SIG-T	TAU R-Z
760	2.435	2.494	0.7581	-10.01	-25.16	-10.08	0.0013
761	0.062	2.494	0.7185	- 9.82	-24.71	- 9.84	0.0011
762	0.187	2.494	0.6929	- 9.88	-24.75	- 9.88	0.0024
763	0.312	2.494	0.6939	- 9.88	-24.76	- 9.88	0.0038
764	0.437	2.494	0.6953	- 9.89	-24.77	- 9.89	0.0051
765	0.562	2.494	0.6972	- 9.89	- 4.78	- 9.90	0.0063
766	0.678	2.494	0.6996	- 9.90	-24.79	- 9.90	0.0072
767	0.811	2.494	0.7024	- 9.90	-24.81	- 9.91	0.0081
768	0.936	2.494	0.7055	- 9.91	-24.83	- 9.92	0.0088
769	1.061	2.494	0.7092	- 9.92	-24.85	- 9.93	0.0092
770	1.186	2.494	0.7131	- 9.93	-24.88	- 9.95	0.0093
771	1.311	2.494	0.7172	- 9.94	-24.91	- 9.96	0.0093
772	1.426	2.494	0.7216	- 9.95	-24.93	- 9.97	0.0090
773	1.561	2.494	0.7262	- 9.95	-24.96	- 9.99	0.0086
774	1.686	2.494	0.7308	- 9.96	-24.99	-10.00	0.0079
775	1.811	2.494	0.7355	- 9.97	-25.02	-10.02	0.0070
776	1.936	2.494	0.7402	- 9.98	-25.05	-10.03	0.0060
777	2.060	2.494	0.7449	- 9.99	-25.08	-10.05	0.0048
778	2.185	2.494	0.7495	- 9.99	-25.11	-10.06	0.0035
779	2.310	2.494	0.7540	-10.00	-25.14	-10.08	0.0022
780	2.435	2.494	0.7585	-10.01	-25.17	-10.09	0.0007
781	0.062	2.494	0.7184	- 9.83	-24.70	- 9.85	0.0004
782	0.187	2.494	0.6928	- 9.88	-24.75	- 9.89	0.0008
783	0.312	2.494	0.6938	- 9.89	-24.75	- 9.89	0.0013
784	0.437	2.494	0.6952	- 9.89	-24.76	- 9.89	0.0017
785	0.562	2.494	0.6971	- 9.89	-24.78	- 9.90	0.0021
786	0.687	2.494	0.6995	- 9.90	-24.79	- 9.91	0.0024
787	0.811	2.494	0.7023	- 9.91	-24.81	- 9.92	0.0027
788	0.936	2.494	0.7055	- 9.91	-24.83	- 9.93	0.0029
789	1.061	2.494	0.7091	- 9.92	-24.85	- 9.94	0.0030
790	1.186	2.494	0.7130	- 9.93	-24.88	- 9.95	0.0030
791	1.311	2.494	0.7172	- 9.94	-24.91	- 9.96	0.0030
792	1.436	2.494	0.7216	- 9.95	-24.93	- 9.98	0.0029
793	1.561	2.494	0.7262	- 9.96	-24.96	- 9.99	0.0028
794	1.686	2.494	0.7309	- 9.96	-24.99	-10.01	0.0026
795	1.811	2.494	0.7356	- 9.97	-25.02	-10.02	0.0023
796	1.936	2.494	0.7403	- 9.98	-25.05	-10.04	0.0019
797	2.060	2.494	0.7450	- 9.99	-25.08	-10.05	0.0016
798	2.185	2.494	0.7497	- 9.99	-25.11	-10.06	0.0011
799	2.310	2.494	0.7542	-10.00	-25.14	-10.08	0.0007
800	2.435	2.494	0.7587	-10.01	-25.17	-10.09	0.0002

TOTALS

VOLUME

AREA

VOL. STR.

0.9992502

1.9951445

0.0007486

FL.	SG-MX	SG-MN	SIG-O	TAU-O	GM-O*100	E-TAN	G-TAN
760	-10.11	-25.16	15.08	7.13	0.53663	1161.	415.
761	-9.82	-24.71	15.79	7.01	0.50931	1226.	438.
762	-9.88	-24.75	14.84	7.01	0.50910	1226.	438.
763	-9.88	-24.76	14.84	7.01	0.50942	1226.	438.
764	-9.89	-24.77	14.85	7.01	0.50993	1224.	437.
764	-9.89	-24.78	14.85	7.02	0.51062	1223.	437.
766	-9.90	-24.79	14.86	7.02	0.51150	1220.	436.
767	-9.90	-24.81	14.88	7.02	0.51257	1218.	435.
768	-9.91	-24.83	14.89	7.03	0.51382	1214.	434.
769	-9.92	-24.85	14.90	7.04	0.51525	1211.	432.
770	-9.93	-24.88	14.92	7.04	0.51685	1207.	431.
771	-9.94	-24.91	14.93	7.05	0.51858	1203.	430.
772	-9.95	-24.93	14.95	7.06	0.52043	1198.	428.
773	-9.95	-24.96	14.97	7.07	0.52236	1194.	426.
774	-9.96	-24.99	14.99	7.08	0.52436	1189.	425.
775	-9.97	-25.02	15.00	7.08	0.52640	1184.	423.
776	-9.98	-25.05	15.02	7.09	0.52845	1179.	421.
777	-9.99	-25.08	15.04	7.10	0.53050	1175.	420.
778	-9.99	-25.11	15.06	7.11	0.53254	1170.	418.
779	-10.00	-25.14	15.07	7.12	0.53456	1165.	416.
780	-10.01	-25.17	15.09	7.13	0.53658	1161.	415.
781	-9.83	-24.70	14.79	7.01	0.50870	1227.	438.
782	-9.88	-24.75	14.84	7.01	0.50850	1228.	439.
783	-9.89	-24.75	14.84	7.01	0.50883	1227.	438.
784	-9.89	-24.76	14.85	7.01	0.50936	1226.	438.
785	-9.89	-24.78	14.86	7.01	0.51007	1224.	437.
786	-9.90	-24.79	14.87	7.02	0.51098	1222.	436.
787	-9.91	-24.81	14.88	7.02	0.51208	1219.	435.
788	-9.91	-24.83	14.89	7.03	0.51337	1216.	434.
789	-9.92	-24.85	14.90	7.03	0.51484	1212.	433.
790	-9.93	-24.88	14.92	7.04	0.51648	1208.	431.
791	-9.94	-24.91	14.94	7.05	0.51825	1204.	430.
792	-9.95	-24.93	14.95	7.06	0.52014	1199.	428.
793	-9.96	-24.96	14.97	7.07	0.52213	1194.	427.
794	-9.96	-24.99	14.99	7.07	0.52417	1189.	425.
795	-9.97	-25.02	15.01	7.08	0.52624	1185.	423.
796	-9.98	-25.05	15.02	7.09	0.52833	1180.	421.
797	-9.99	-25.08	15.04	7.10	0.53041	1175.	420.
798	-9.99	-25.11	15.06	7.11	0.53248	1170.	418.
799	-10.00	-25.14	15.07	7.12	0.53452	1166.	416.
800	-10.01	-25.17	15.09	7.13	0.53655	1161.	415.

**The vita has been removed from
the scanned document**

FINITE ELEMENT ANALYSIS OF SOIL COMPACTION

by

George Edward Coleman, III

(ABSTRACT)

The problem of predicting soil compaction is one of major concern to those in the agricultural industry. In this investigation the feasibility of using a numerical analysis technique to study force-compaction phenomena in soils was considered. The finite element technique was used to observe compaction in a triaxially loaded soil sample. The stress-strain relationship used for the analysis was a generalized Von Mises yield criterion developed from triaxial test data for prepared Ottawa silica sand samples. An incremental non-linearization technique was employed to approximate this stress-strain relationship.

It was found that soil compaction was dependent upon the mean normal stress and shear stress. The latter had a much greater influence upon compaction, for the range of pressures studied.